

UNIVERSIDAD SAN FRANCISCO DE QUITO USFQ

Colegio de Posgrados

**Design and development of a biosensor for the detection of phenylalanine
and tyrosine based on prokaryotic genetic circuits**

**Mecanismo de Titulación: Tesis en torno a una hipótesis o problema de
investigación y su contrastación**

Christian Benjamín Arias Almeida

**Vanessa Romero Aguilar M.D., Ph.D.
Directora de Trabajo de
Titulación**

Trabajo de titulación de posgrado presentado como requisito
para la obtención del título de Máster en Microbiología

Quito, 20 de Mayo de 2025

UNIVERSIDAD SAN FRANCISCO DE QUITO USFQ
COLEGIO DE POSGRADOS

HOJA DE APROBACIÓN DE TRABAJO DE TITULACIÓN

Design and development of a biosensor for the detection of phenylalanine and tyrosine based on prokaryotic genetic circuits

Christian Benjamín Arias Almeida

Nombre del Director del Programa:	Patricio Rojas-Silva
Título académico:	M.D., Ph.D.
Director del programa de:	Maestría en Microbiología

Nombre del Decano del colegio Académico:	Carlos Valle
Título académico:	Ph.D.
Decano del Colegio:	COCIBA

Nombre del Decano del Colegio de Posgrados:	Dario Niebieskikwiat
Título académico:	Ph.D

Quito, 20 de mayo de 2025

© DERECHOS DE AUTOR

Por medio del presente documento certifico que he leído todas las Políticas y Manuales de la Universidad San Francisco de Quito USFQ, incluyendo la Política de Propiedad Intelectual USFQ, y estoy de acuerdo con su contenido, por lo que los derechos de propiedad intelectual del presente trabajo quedan sujetos a lo dispuesto en esas Políticas.

Asimismo, autorizo a la USFQ para que realice la digitalización y publicación de este trabajo en el repositorio virtual, de conformidad a lo dispuesto en la Ley Orgánica de Educación Superior del Ecuador.

Nombre del estudiante: Christian Benjamin Arias Almeida

Código de estudiante: 00331859

C.I.: 1716792047

Lugar y fecha: Quito, de mayo de 2025.

ACLARACIÓN PARA PUBLICACIÓN

Nota: El presente trabajo, en su totalidad o cualquiera de sus partes, no debe ser considerado como una publicación, incluso a pesar de estar disponible sin restricciones a través de un repositorio institucional. Esta declaración se alinea con las prácticas y recomendaciones presentadas por el Committee on Publication Ethics COPE descritas por Barbour et al. (2017) Discussion document on best practice for issues around theses publishing, disponible en <http://bit.ly/COPETheses>

UNPUBLISHED DOCUMENT

Note: The following graduation project is available through Universidad San Francisco de Quito USFQ institutional repository. Nonetheless, this project – in whole or in part – should not be considered a publication. This statement follows the recommendations presented by the Committee on Publication Ethics COPE described by Barbour et al. (2017) Discussion document on best practice for issues around theses publishing available on <http://bit.ly/COPETheses>.

TABLE OF CONTENTS

DEDICATION.....	6
ACKNOWLEDGEMENTS	7
RESUMEN	8
ABSTRACT	9
TABLE INDEX	10
FIGURES INDEX	11
INTRODUCTION	13
LITERATURE REVIEW	18
METHODS AND STUDY DESING	23
Literature review.....	23
Genetic circuits construction.....	24
System induction.....	38
RESULTS AND DISCUSSION.....	39
CONCLUSIONS	49
REFERENCES	50

DEDICATION

To my mother Ivonne, who has never stopped supporting me and watching me grow,
to my sister Nicole, who has always been there when I needed her,
to my husband Nicolas, who has tirelessly been that support throughout this last 5 years and has
known how to help me being stronger when I have doubted my abilities,
and to all of us who seek an opportunity to shine, as GFP, in science.

ACKNOWLEDGEMENTS

I would like to thank my director, Vanessa Romero, for believing in my crazy ideas and my potential, and for continuing to support me every day to develop not only as a professional but also as a person, making me wiser and more skilled in science. I would like to thank my tutor Juan Carlos Collantes for always helping me find a way to achieve the desired designs, always supporting me, seeing the potential in me and searching different ways to see me grow. I would like to thank my tutor Gabriel Trueba for agreeing to be part of my committee and always providing positive comments for the improvement of this project.

I would also like to thank USFQ for the funding used in this research and the CEDIA corporation for being the largest beneficiary of this project by giving us the “I+D+I” and “Registra” 2023 funds. Without their financial support, this research would not have been possible.

RESUMEN

El desarrollo de biosensores para la detección de fenilalanina y tirosina es fundamental para mejorar las capacidades de diagnóstico y monitoreo de trastornos metabólicos como la fenilcetonuria (PKU). Este estudio se centra en el diseño y la construcción de un sistema novedoso de biosensores basado en circuitos genéticos procariotas. Al emplear el factor de transcripción TyrR, ARN antisentido (asRNA) y sistemas STAR (Small Transcription Activating RNA), el biosensor logra una detección y cuantificación precisas de estos aminoácidos. El biosensor de fenilalanina utiliza el promotor *ptyrP* con un reportero fluorescente rojo cromogénico, mientras que el biosensor de tirosina emplea el promotor *paroF* en combinación con la tecnología STAR para obtener una señal verde fluorescente, directamente proporcional a la concentración del aminoácido. Ambos sistemas mostraron una fuerte correlación lineal con concentraciones fisiológicas relevantes de aminoácidos, validando su potencial como herramientas de diagnóstico. Esta investigación representa un paso prometedor hacia el desarrollo de biosensores accesibles y rentables para aplicaciones clínicas y de campo.

Palabras clave: biosensores, detección de fenilalanina, detección de tirosina, factores de transcripción, ARN antisentido, sistema STAR, fenilcetonuria (PKU), diagnóstico de PKU, trastornos metabólicos.

ABSTRACT

The development of biosensors for the detection of phenylalanine and tyrosine is critical for improving diagnostic and monitoring capabilities for metabolic disorders such as Phenylketonuria (PKU). This study focuses on the design and construction of a novel biosensor system based on prokaryotic genetic circuits. By leveraging transcription factor TyrR, antisense RNA (asRNA), and STAR (Small Transcription Activating RNA) systems, the biosensor achieves precise detection and quantification of these amino acids. The phenylalanine biosensor uses the *ptyrP* promoter with a chromogenic red fluorescence reporter, while the tyrosine biosensor utilizes the *paroF* promoter in combination with STAR technology to achieve a green fluorescent output directly proportional to the concentration of the amino acids. Both systems demonstrated a strong linear correlation with relevant physiological amino acid concentrations, validating their potential as diagnostic tools. This research represents a promising step toward developing accessible, cost-effective biosensors for clinical and field applications.

Keywords: biosensors, phenylalanine detection, tyrosine detection, transcription factors, antisense RNA, STAR system, PKU diagnostics, metabolic disorders.

TABLE INDEX

Table 1. Biological parts used in the study

Table 2. Results of asrna designed against amilgfp cassette

Table 3. Primer sequences used in this study

Table 4. Phenylalanine and tyrosine levels in normal and pku patients

FIGURES INDEX

Figure 1. Different bio-parts of the biosensor for Phe and tyr detection.

Figure 2. *MODULE F + R* behavior.

Figure 3. *MODULE T + R* behavior.

Figure 4. History of *in-vitro* construction of Module F

Figure 5. History of *in-vitro* construction of Module T

Figure 6. History of *in-vitro* construction of Module R

Figure 7. asRNA binding sites for regulation of *STAR-amilGFP* expression cassette.

Figure 8. Sanger sequencing confirmation of *as1.amilGFP* cloning.

Figure 9. Sanger sequencing confirmation of *as.STAR* regulator cloning.

Figure 10. Desing and function of *STAR regulator* sequence.

Figure 11. Confirmation of DNA assembly by restriction enzyme digestion.

Figure 12. Neighborhood of selected restriction sites in *MOD T* plasmid.

Figure 13. Phenylalanine induction with the Phe-biosensor (*MOD F + MOD R*).

Figure 14. Tyrosine induction with the Tyr-biosensor (*MOD T + MOD R*).

INTRODUCTION

Background.

The evolution of biosensor technology has been driven by the need for more efficient, accurate, and user-friendly diagnostic tools, particularly for the detection of small molecules such as amino acids. These biomolecules play crucial roles in various metabolic pathways; thus, their abnormal levels can be used as biomarkers indicative of metabolic disorders. Among these, Phenylketonuria (PKU) is caused by mutations in the *PAH* gene which encodes phenylalanine hydroxylase (PAH) enzyme. This enzyme is critical for converting phenylalanine into tyrosine, precursor of the catecholamine neurotransmitters such as dopamine, epinephrine and norepinephrine, and the lack of functional PAH leads to the accumulation of toxic levels of phenylalanine in the blood and brain tissue, which, if uncontrolled, can cause severe intellectual disabilities, developmental delays, and other neurological impairments (Nelwan, 2020). Proper control is crucial, typically achieved through newborn screening programs using High-Performance Liquid Chromatography (HPLC) to measure phenylalanine levels (Haghighi et al., 2015). While effective, this method is limited by its high cost, need for sophisticated equipment, requirement for specialized personnel and turnaround time to obtain the results.

There is a growing interest in developing alternative diagnostic tools that are more accessible, especially in low-resource settings. Biosensors have emerged as a promising solution, offering advantages such as real-time monitoring, ease of use, portability, lower costs, and faster turnaround times to obtain results. Recent advancements in synthetic biology and biosensors have enabled the creation of technologies that design genetic circuits, that are constructs with DNA parts capable of performing a specific function, response through transcription and translation, to sense specific molecules. This has been achieved by mixing reporter proteins and biological recognition elements, such as protein based transcriptional factors, to create whole-cell biosensors capable of detecting and quantifying analytes ranging from metals like zinc to amino acids like phenylalanine (Phe) and tyrosine (Tyr), but in an impractical manner. This genetic circuits depend

on the nature of promoters, in this way if a promoter have a positive repressive or a negative inductive nature, they cannot be used as a final product cause in this way consumers will need to make a inversive correlation between the output and what had been sensed (M. Guo et al., 2019a; Lin et al., 2018a; Navani et al., 2021; Roy et al., 2021; Watstein & Styczynski, 2018). Antisense RNAs (asRNA) can be harnessed for regulating, and even completely reversing genetic circuits that rely on promoters that gives a inversely proportional expression. These synthetic sequences are designed to be complementary to specific sequences of mRNA targets, thereby exerting gene silencing by regulating gene expression by binding to the mRNA and preventing its translation. In the context of biosensors, these antisense RNA molecules can be engineered to specifically target the mRNA of a reporter gene, silencing its expression (Lee et al., n.d., 2019). This approach is particularly advantageous because it offers high specificity and sensitivity, as this kind of constructs can be used to control the expression of genetic circuits in a biosensor system in specific ways.

Here, we use RNA technology for development of a genetic circuit that uses a transcriptional factor as a central unit processor (CPU) to respond to multiple signals. This CPU is the tyrR protein form the Tyr Operon system and have different domains that allows the protein to bind aromatic amino acids and DNA sequences (Tyr boxes) (Bai et al., 2019a; Mahr et al., 2016; Pittard et al., 2005). TyrR binds to phenylalanine (Phe), promoting its dimerization and activation of transcription as a transcriptional activator of the tyrP channel. On the other hand, binding to tyrosine promotes the formation of a hexamer of tyrR proteins that acts as a repressor of the aroF enzyme. These different functionalities from a single protein are due to the genetic architecture that the *tyr boxes* had in the promoter regions of the genes inside the Tyr Operon (Pittard et al., 2005). We use these two promoters to make a biosensor that respond to Phe and Tyr concentrations, and in the case of the use of *aroF* promoter, since its nature is being a repressor we use asRNA and the STAR system to tune up the circuit and enhance Tyr sensing.

This research not only addresses the limitations of traditional diagnostic methods but also opens new avenues for continuous monitoring of PKU and other metabolic disorders. By enabling

real-time detection and providing immediate feedback, biosensors could facilitate more dynamic and personalized management of PKU, ultimately improving patient outcomes (Lin et al., 2018; Rifai et al., 2017).

Justification of the Study.

The need for accessible and reliable diagnostic tools for metabolic disorders, particularly PKU, cannot be overstated. Current diagnostic protocols, while effective in developed regions, are less feasible in resource-limited settings due to the high cost, complexity, and infrastructure requirements of methods like HPLC (Wilson et al., 2005). The global burden of PKU underscores the necessity for innovative solutions that are both cost-effective and scalable, capable of reaching low-income populations where early diagnosis and treatment are critical (Aguirre et al., 2024).

Due to restricted access to specialized healthcare infrastructure and resources, managing PKU is especially difficult in Ecuador. Implemented since 2012, the nationwide newborn screening (NBS) program has encountered numerous challenges, such as uneven coverage, particularly in rural areas, and delays in test results, which can occur up to three months after sample collection (Aguirre et al., 2024). Particularly in infants, where early intervention is crucial, this delay in diagnosis and monitoring can result in irreversible neurological damage. As patients and carers frequently rely on international guidelines that might not take local dietary habits and food availability into account, the absence of regional databases describing the phenylalanine (Phe) content in foods further complicates dietary management. Additionally, there is limited access to low-protein foods and supplement formulas, and many families may find the price of these products prohibitive.

The current reliance on centralized laboratory testing in Ecuador poses serious obstacles to the effective management of PKU, making the need for a biosensor that can monitor Phe and tyrosine (Tyr) levels in real-time especially pressing. Patients would be able to keep an eye on their Phe levels at home with a portable biosensor, which would eliminate the need for frequent trips to medical facilities and allow for prompt dietary changes. In rural areas, where access to healthcare

services is limited and travelling to urban centers for testing can be prohibitively expensive and time-consuming, this would be especially helpful. A biosensor might fill the gap in PKU care by offering an affordable and easily accessible solution, guaranteeing that patients in settings with limited resources receive the prompt and accurate monitoring required for efficient disease management.

This study is justified by the gap between the efficacy of existing PKU diagnostic methods and their accessibility. While HPLC remains a reliable method for PKU screening, its application is largely confined to centralized laboratories due to the need for sophisticated equipment and skilled technicians. This centralization creates a bottleneck in the diagnostic process, delaying critical interventions in the early stages of PKU, where timely treatment is essential.

Moreover, there is a significant demand for tools that allow for continuous monitoring rather than periodic testing. The management of PKU typically involves strict dietary control, with the patient's phenylalanine intake needing constant adjustment (Brown & Guest, 1999; Nelwan, 2020; Rampini et al., 1974). Fluctuations in phenylalanine levels can occur rapidly, demanding diagnostic tools that provide real-time feedback. A biosensor designed for this purpose could significantly enhance patient compliance and treatment efficacy by enabling more frequent and convenient monitoring (K. H. Guo et al., 2018).

The biosensor proposed in this study leverages the specificity of engineered transcription factors and antisense RNA molecules, integrated with either electrochemical or optical detection systems, which is crucial for achieving the desired sensitivity and specificity. The engineered genetic circuit developed here uses transcription factors to bind phenylalanine or tyrosine with high selectivity, while antisense RNA allows to transform a repressive signal into an expression signal. In this way, the transcriptional factor used was the TyrR protein, that acts as the central processor unit of the Tyr Operon. The TyrR protein have the capability of present different conformation depending on the aminoacidic in the media. Phenylalanine binds between two isomeric structures, making a dimer capable of jointing to the *tyrR* promoter and activate its expression. This promoter contains an arrangement of two *tyr boxes* one strong and one weak next to the -35 and -10 regions. The

architecture of *ptyrP* allows the TyrR dimer to bind and activate the transcription by the recruitment of the sigma factor by joining at its α subunit. At the other hand TyrR protein performs a repressor function when tyrosine is present in media. In this way, tyrosine binds to TyrR protein and allows the formation of a hexameric structure. This TyrR hexamer can join at the *aroF* promoter by binding at the *tyr* boxes in this region. This *paroF* present an architecture of two strong boxes and one weak box allowing the TyrR-hexamer to bind and bend DNA around it to perform a physical block preventing polymerase to attach. Since the nature of this promoter is a negative induction with tyrosine signal, a mechanism to invert the nature of induction was needed to engineer. For this an antisense RNA system was designed and couple to the expression of a protein reporter and asRNA designer molecules. The integration of these biological components with an appropriate transduction mechanism ensures that the biosensor can translate molecular interactions into semi quantifiable signals.

The availability of this biosensor in low-resource settings could allow access to PKU screening and monitoring, addressing healthcare disparities across different regions. By reducing dependence on complex equipment and highly trained personnel, this biosensor could bring reliable diagnostic capabilities to communities that currently lack access to such technologies. The potential impact of this research extends beyond PKU, as the principles and methods developed here could be adapted for other metabolic disorders or even different types of biomarkers.

Research Objectives.

General Objective.

To develop and validate a biosensor based on prokaryotic genetic circuits for the detection of phenylalanine and tyrosine, with the aim of improving the management of Phenylketonuria (PKU).

Specific Objectives.

1. To design and engineer *Escherichia coli* K-12 transcription factor-based detection systems with high specificity for phenylalanine and tyrosine detection.
2. To integrate these detection systems with an appropriate signal transduction mechanism

like RNA technology, to have directly proportional measurements and readout with fluorescence/colorimetry.

3. To validate the biosensor's performance with a range of known concentrations of phenylalanine and tyrosine.

Hypothesis.

A biosensor employing transcription factors derived from *E. coli* genome and engineered antisense RNA molecules will exhibit biologically relevant sensitivity for the detection of phenylalanine and tyrosine, offering a practical solution for PKU detection and monitoring in a future.

Theoretical Framework.

This study is based on the principles of molecular recognition and signal transduction in biological systems. The engineered genetic circuit based on transcription factors and antisense RNA molecules were designed based on in-silico design, protein-ligand binding and asRNA design principles previous studies, ensuring a functional design for target amino acids and activating expression as a result. This allows the biosensor to have the ability to generate a measurable signal in response to ligand binding.

LITERATURE REVIEW

This review centers on the development and application of biosensors for detecting amino acids like phenylalanine and tyrosine, which are crucial for managing metabolic disorders like Phenylketonuria (PKU). Phenylketonuria is a rare genetic disease that is inherited in an autosomal recessive way, and it is caused by more than 80 characterized mutations in the phenyl alanine hydroxylase enzyme (PAH) gene. Depending on the specific mutations in this gene, patients tend to present different levels of enzyme deficiency, impacting the metabolic kinetics of phenylalanine ingested from diet (Nelwan, 2020). This impairment in untreated or undiagnosed patients cause

severe neurological and skin pigmentation deficiencies complications. The main interventions for this disease are nutritional management accompanied with constant monitoring to control the amino acid levels in the body (Castro et al., 2012; Matalon & Michals, 1991; MedlinePlus, 2017; van Spronsen et al., 2021). This makes crucial the development of analytical techniques for the control of these patients, and in this manner the search for more portable and accessible methods. Considering these new techniques, here we examine the advancements in biosensor technology, emphasizing systems that use antisense RNA (asRNA) molecules and transcription factors. Here, we also address the diversity of chromogenic reporters, the limitations of traditional diagnostic tools, particularly High-Performance Liquid Chromatography (HPLC), and how recent innovations in biosensors may overcome these challenges. We identify existing research gaps, shedding light on the unique contributions this investigation aims to provide.

Traditional Diagnostic Methods for PKU.

High-Performance Liquid Chromatography (HPLC) remains the gold standard for detecting phenylalanine in biological samples, like blood and urine (Haghighi et al., 2015). It is widely accepted for its accuracy and reliability in measuring amino acid levels in blood samples, making it vital for newborn screening programs (van Spronsen et al., 2021). However, despite its effectiveness, HPLC's high costs, complexity, and need for specialized equipment and personnel limit its use in low-income countries, such as Ecuador. Moreover, HPLC offers only a snapshot of phenylalanine levels, missing metabolic fluctuations that may occur due to the genetic deficiency of the PAH enzyme or biological variability (American College of Medical Genetics, 2009; Mihali et al., 2018). These limitations have driven the development for more portable, faster and cost-effective diagnostic tools capable of continuous monitoring of these patients.

Advancements in Biosensor Technology for Amino Acid Detection.

Biosensors have emerged as promising alternatives to conventional diagnostics, offering portability, lower costs, and real-time monitoring capabilities. These devices rely on biological

recognition elements that interact with specific molecules to generate detectable signals. Here we summarize the latest developments in biosensors, particularly those utilizing asRNA molecules and transcription factors.

Antisense RNA-Based Circuits.

Antisense RNA molecules are RNA sequences complementary to specific target RNAs, and in nature they regulate global gene expression, transcription, translation and in some cases other biological process (Chappell et al., 2013). Scientists have produced asRNA molecules that are designed with preset rules that take into account the localization of the target sequences within the mRNA target, the total energy of the asRNA/mRNA complex, the effects mismatches, the length of the asRNA and the addition of regulatory sequences (e.g. Hfq sites for enhancing RNA degradation mediated by RNase E) in its 3' end (Chappell et al., 2013; Hoynes-O'Connor & Moon, 2016a; Lee et al., 2019; Vogel & Luisi, 2011). The latter elements are designed to block translation and regulate gene expression. One promising technology based on the design of asRNA against regulatory structures like terminators is the STAR technology (Small Transcriptional Activating RNAs) (Chappell et al., 2015; Meyer et al., 2015). The STAR is a two-component system: one expression cassette that locates a termination sequence between the promoter and the coding sequence (CDS), and an asRNA sequence (STAR regulator) against the 5' stem loop of the terminator. When the STAR regulator is present, this sequence binds to the terminator and destabilizes its structure, thus its linearization activates the transcription (Chappell et al., 2015). In this way asRNA and the STAR system integration allows to tune up the genetic circuit and invert the induction signal from a negative to a positive performance.

Transcription Factor-Based Biosensors.

Transcription factor-based biosensors have gained significant attention for their capacity to detect specific molecules like amino acids or metabolic byproducts with high precision. These biosensors can use transcription factors that bind to target molecules and modulate gene expression, enabling

the detection of analytes in diverse settings. Lin et al. (2018) developed a biosensor utilizing the tyrR transcription factor from *Escherichia coli* to regulate fluorescent protein expression in response to phenylalanine and tyrosine levels. This system demonstrated high specificity and sensitivity, facilitating accurate amino acid quantification in human blood and urine samples in relevant physiological ranges (Phe: 5 – 1000mM; tyr: 5 – 100mM). Such biosensors are particularly promising for diagnosing and monitoring metabolic disorders like PKU. As previously mentioned, the problem with the existing biosensors based on tyrR protein system is the inversely proportional fluorescence that is emitted in presence of tyrosine, which makes it an impractical system to be use in a commercial, patient-centered settings (Bai et al., 2019b; Lin et al., 2018a). Other biosensors based on transcriptional factors have been widely developed. For instance, Guo et al. (2019) designed biosensors using the MerR family of transcription factors. These proteins acted as “rheostats”, allowing the detection through customizable promoter designs (M. Guo et al., 2019b). The aim of this research was to obtain a biosensor for heavy metal detection. Roy et al. (2021) expanded on transcription factor-based biosensing by creating programmable multiplexed systems (Roy et al., 2021). Their whole-cell biosensors used genetic circuits to achieve ultra-sensitive detection of aromatic pollutants, like phenols and benzene. The modularity of their platform highlights its potential adaptability for metabolic analytes such as phenylalanine and tyrosine. These approaches exemplify how transcription factors can provide robust solutions for environmental and clinical diagnostics.

Chromogenic Reporters.

Chromogenic reporters derived from fluorescent proteins offer a visually intuitive output for biosensing applications, which are particularly useful in low-resource environments. Depending on the gene used, these proteins produce distinct colors upon activation, eliminating the need for sophisticated detection equipment. Liljeruhm et al. (2018) engineered a palette of chromoproteins, enabling their application in bacterial biosensors. By optimizing these proteins for expression in *E. coli*, they facilitated the development of tools that provide clear colorimetric outputs, making

them ideal for field diagnostics (Liljeruhm et al., 2018). Similarly, Alieva et al. (2008) explored coral fluorescent proteins, uncovering a variety of spectrally distinct chromoproteins. These proteins were adapted for use as chromogenic reporters in biosensors, offering robust performance in diverse biological settings (Bao et al., 2020; Liljeruhm et al., 2018). Their intrinsic ability to produce color without external cofactors simplifies their integration into biosensor systems.

Challenges and Gaps in Research.

Despite considerable advancements, significant challenges remain in the development of biosensors based on transcription factors, antisense RNA (asRNA), and chromogenic reporters. Transcription factor-based biosensors, such as those developed by Lin et al. (2018) and Guo et al. (2019), demonstrate high specificity but require enhancements in stability under variable conditions and scalability for practical, real-world applications. Furthermore, the challenge of multiplexing these systems to detect multiple analytes simultaneously, as highlighted by Roy et al. (2021), persists due to issues with cross-reactivity. Biosensors with RNA bio parts, including systems such as STAR (Small Transcription Activating RNA) and antisense RNA, will offer precise control of gene expression by giving orthogonality and recoding the nature of the negative inducible signals. However, further research is needed to improve their efficiency, reliability, and compatibility with clinical samples, particularly in complex biological environments. Chromogenic reporters, while cost-effective and straightforward to use and detect, continue to face limitations in sensitivity and dynamic range. Systems like those developed by Liljeruhm et al. (2018) and Alieva et al. (2008) have demonstrated potential but require optimization to expand their applicability across diverse scenarios. Thus, the present work search for the development of a biosensor capable of quantification of phenylalanine/tyrosine and the emission of a direct proportional fluorescent and chromogenic signal. For this, concepts and bio part previously mentioned like the *tyrR* protein, STAR system and antisense RNA will be joined together top engineered a more sensible and specific genetic circuit capable of being used as a biosensor in a biomedical context.

Summary and Conclusions.

This review emphasizes significant advancements in biosensor technologies, focusing on transcription factor-based systems, antisense RNA circuits, and chromogenic reporters. Transcription factor-based biosensors, exemplified by Lin et al. (2018) and Dhyani et al. (2021), enable accurate detection of amino acids and other metabolic biomarkers. RNA-based systems, such as STAR, introduce a layer of flexibility and tunability in biosensor design, making them suitable for applications requiring complex gene regulation. Chromogenic reporters, such as those designed by Liljeruhm et al. (2018), offer intuitive, visually interpretable outputs, positioning them as ideal candidates for field diagnostics. Despite these promising developments, critical challenges persist in improving the robustness, sensitivity, specificity and scalability of these technologies. A synergistic approach that combines the precision of transcription factor biosensors, the adaptability of RNA-based systems, and the simplicity of chromogenic reporters could lead to the creation of powerful, versatile diagnostic tools for use in both clinical and environmental contexts.

METHODS AND STUDY DESING

Literature review.

The literature reviewed for this analysis was carefully selected through a comprehensive search using Google Scholar. The search focused on peer-reviewed articles, conference proceedings, and book chapters from the past two decades, using keywords such as "biosensors," "phenylalanine detection," "tyrosine biosensor," "antisense RNA," "transcription factor biosensors," and "PKU diagnostics." The inclusion criteria prioritized works relevant to biosensor technology, experimental validation, and their clinical applications, particularly in PKU diagnostics.

Genetic circuits construction.***In-silico: System Design and Construction.***

For system design and rationalization of the different parts needed, we searched for biological parts in the literature that allow us to create a DNA construct capable of detecting phenylalanine and tyrosine at the same time (Table 1 and Figure 1-3). The Tyr Operon was chosen as the main component of the system for development of the biosensor. The TyrR protein, that works as the CPU of the system, have the capability of recognize and translate signals from aromatic amino acids into transcriptional signals. As previously described this system have different promoters that control the expression of different genes involve in the regulation of aromatic amino acid metabolism. This biosensor is based on what we call *tyr boxes*, this DNA regions that can be bound by multiple conformations of TyrR. These sequences are designed at different conformations so the regulatory protein can bind different promoters in a specific and selective way. This binding at different conformations allows the protein TyrR to respond differently with upon binding to different amino acids, such as Phe or Tyr.

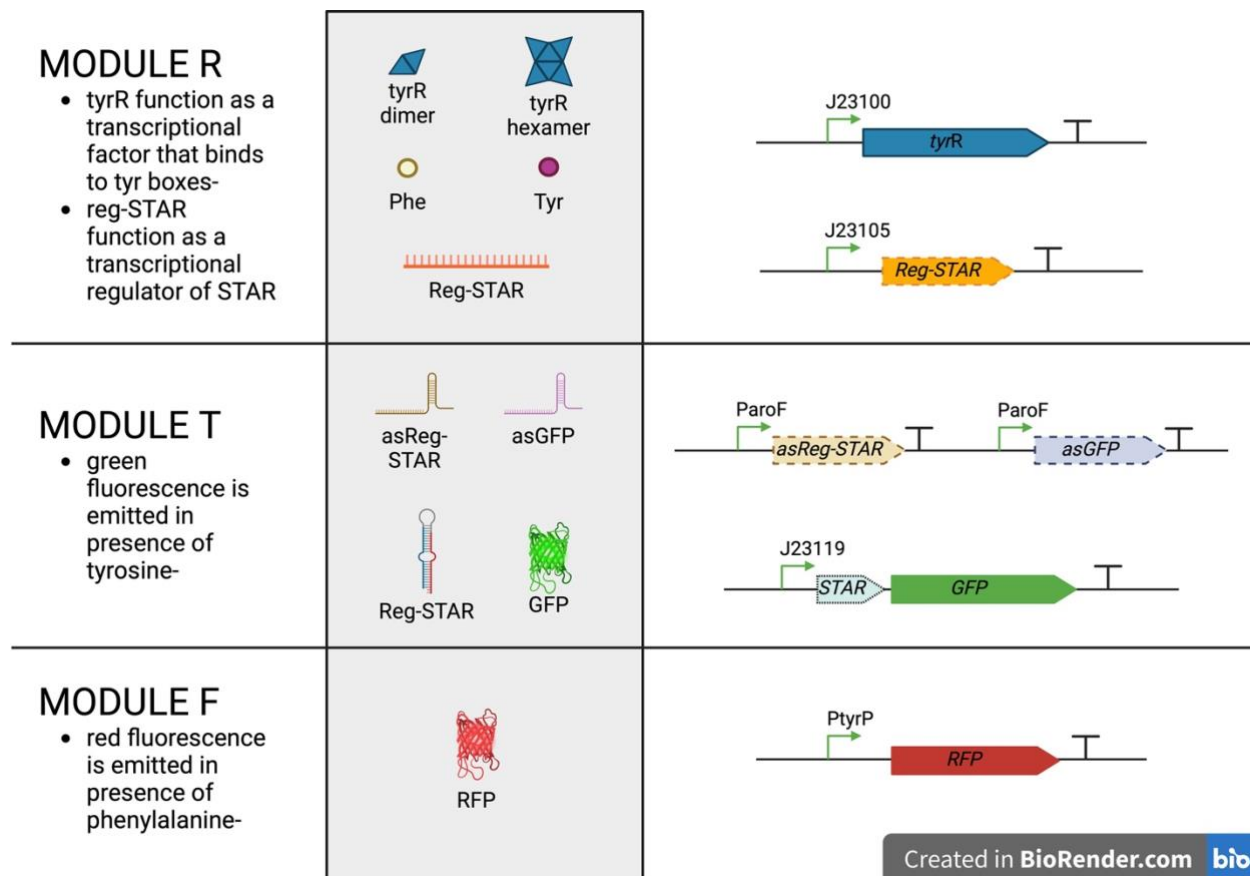


Figure 1. Different bio-parts of the biosensor for Phe and tyr detection. Different bioparts that conform the functional DNA modules. MOD R(Regulator) have the regulatory molecules of the system such as the STAR regulator (Reg-STAR) and the tyrR protein. MOD T (Tyrosine) are formed by the asRNA circuits, *paroF* promoter and the green fluorescent protein (GFP) *amilGFP* as reporter to sense tyrosine concentrations. MOD F (Fenilalanina) are formed by the *ptyrP* promoter and the red fluorescent (RFP) protein *efordRed* as reporter to sense phenylalanine concentrations.

TABLE 1. BIOLOGYCAL PARTS USED IN THE STUDY

Bio-part	DNA Sequence	Reference
<i>TyrR</i>	ATGCGTCTGGAAGTCTTTTGTGAAGACCGACTCGGTC TGACCCGCGAATTACTCGATCTACTCGTGCTAAGAGG CATTGATTACGCGGTATTGAGATTGATCCCATTGGG	(Lin et al., 2018b)

CGAATCTACCTCAATTTTGCTGAACTGGAGTTTGAGA
GTTTCAGCAGTCTGATGGCCGAAATACGCCGTATTGC
GGGTGTTACCGATGTGCGTACTGTCCCGTGGATGCCT
TCCGAACGTGAGCATCTGGCGTTGAGCGCGTTACTGG
AGGCGTTGCCTGAACCTGTGCTCTCTGTCGATATGAA
AAGCAAAGTGGATATGGCGAACCCGGCGAGCTGTCA
GCTTTTTGGGCAAAAATTGGATCGCCTGCGCAACCAT
ACCGCCGCACAATTGATTAACGGCTTTAATTTTTTAC
GTTGGCTGGAAAGCGAACCGCAAGATTCGCATAACG
AGCATGTCGTTATTAATGGGCAGAATTCCTGATGGA
GATTACGCCTGTTTATCTTCAGGATGAAAATGATCAA
CACGTCCTGACCGGTGCGGTGGTGATGTTGCGATCAA
CGATTCGTATGGGCCGCCAGTTGCAAAAATGTCGCCGC
CCAGGACGTCAGCGCCTTCAGTCAAATTGTCGCCGTC
AGCCCGAAAATGAAGCATGTTGTCGAACAGGCGCAG
AAACTGGCGATGCTAAGCGCGCCGCTGCTGATTACGG
GTGACACAGGTACAGGTAAAGATCTCTTTGCCTACGC
CTGCCATCAGGCAAGCCCCAGAGCGGGCAAACCTTA
CCTGGCGCTGAACTGTGCGTCTATACCGGAAGATGCG
GTCGAGAGTGAACTGTTTGGTCATGCTCCGGAAGGGA
AGAAAGGATTCTTTGAGCAGGCGAACGGTGGTTCGG
TGCTGTTGGATGAAATAGGGGAAATGTCACCACGGA
TGCAGGCGAAATTACTGCGTTTCCTTAATGATGGCAC
TTCCGTCGGGTGGCGAAGACCATGAGGTGCATGTC
GATGTGCGGGTGATTTGCGCTACGCAGAAGAATCTGG
TCGAACTGGTGCAAAAAGGCATGTTCCGTGAAGATCT

	CTATTATCGTCTGAACGTGTTGACGCTCAATCTGCCG	
	CCGCTACGTGACTGTCCGCAGGACATCATGCCGTAA	
	CTGAGCTGTTCTGTCGCCCCGCTTTGCCGACGAGCAGGG	
	CGTGCCGCGTCCGAAACTGGCCGCTGACCTGAATACT	
	GTACTIONACGCGTTATGCGTGGCCGGGAAATGTGCGGC	
	AGTTAAAGAACGCTATCTATCGCGCACTGACACAAC	
	GGACGGTTATGAGCTGCGTCCACAGGATATTTTGTTG	
	CCGGATTATGACGCCGCAACGGTAGCCGTGGGCGAA	
	GATGCGATGGAAGGTTCTGCTGGACGAAATCACCAGC	
	CGTTTTGAACGCTCGGTATTAACCCAGCTTTATCGCA	
	ATTATCCCAGCACGCGCAAACCTGGCAAAACGTCTCGG	
	CGTTTCACATACCGCGATTGCCAATAAGTTGCGGGAA	
	TATGGTCTGAGTCAGAAGAAGAACGAAGAGTAA	
<i>STARsequence</i>	AGTTTTTACAGTGAATTGTTTTAATTAGTTGTATAAAT	(Meyer,
<i>AD1.A5</i>	GTTGGAGCAGCGGGGAATGTATACAGTTCATGTATAT	2015)
	ATTCCCCGCTTTTTTTTTT	
<i>STAR regulator</i>	TGAACTGTATACATTCCCCGCTGCTCCAACATTTATA	(Meyer,
<i>AD1.S5</i>	CAACTAATTAACAATTCACTGTAAAAACT	2015)
<i>As.reg-STAR</i>	GTTGTATAAATGTTGGAGCAGCGGGGAATGTATACA	(Meyer,
	GTTCA	2015)
<i>paroF</i>	AGGGAGTGTAATTTATCTATACAGAGGTAAGGGTTG	(Lin et al.,
	AAAGCGCGACTAAATTGCCTGTGTAAATAAAAAATGT	2018b)
	ACGAAATATGGATTGAAAACCTTTACTTTATGTGTTAT	
	CGTTACGTCATCCTCGCTGAGGATCAACTATCGCAAA	
	CGAGCATAAACAGGATCGCCATC	

<i>ptyrP</i>	GCCTAGCGTAGCGATTGCCGCTTATGAAGACTTTGCG CCAGCGCAGGACTGAATGCTTTTTATTGTACATTTAT ATTTACACCATATGTAACGTCGGTTTGACGAAGCAGC CGTTATGCCTTAACCTGCGCCGCAGATATCACTCATA AAGATCGTCAGGACAGAAGAAAGC	(Lin et al., 2018b)
<i>MicF</i>	TCATTTCTGAATGTCTGTTTACCCCTATTTCAACCGGA TGCCTCGCATTCGGTTTTTTTTT	

For this design, we selected the promoters *ptyrP* and *paroF* for their capability of react to phenylalanine and tyrosine, respectively. Promoter *ptyrP*, works as a transcriptional activator that allows the recruitment of a sigma factor by joining to its α subunit, and subsequently to the RNA polymerase leading to transcription activation. We placed the efordRed reporter under the control of the *ptyrP* promoter, which is a chromogenic protein that is capable of fluorescent and colorimetric emission (Figure 2). The use of the *paroF* promoter was more challenging for use as an activator of reporter expression, since its nature is being a repressor of transcription. To tackle this challenge, we looked for a mechanism by which we can translate the signal and obtain a read-out directly proportional to the detected metabolite (i.e. promoting reporter gene expression instead of repressing it). We explored the use of STAR system from the *Enterococcus faecalis* *pDAI* plasmid, an intermediate system that can allows to translate this signal into an upregulated one with the integration of antisense RNAs (Clewell, 2007). This system includes a STAR sequence that acts as a premature terminator and prevents the transcription of the mRNA fused to the STAR sequence, and a STAR regulator that acts as an asRNA regulator molecule that binds to the STAR sequence destabilizing their hairpin structure on the terminator. This allows us to place the amilGFP reporter under the control of the STAR sequence. This STAR-amilGFP design is also under the control of the constitutive promoter *J23119*, and the STAR regulator is controlled by

the *J23105* promoter. In this way, when the STAR regulator is present, the expression of *amilGFP* would be activated.

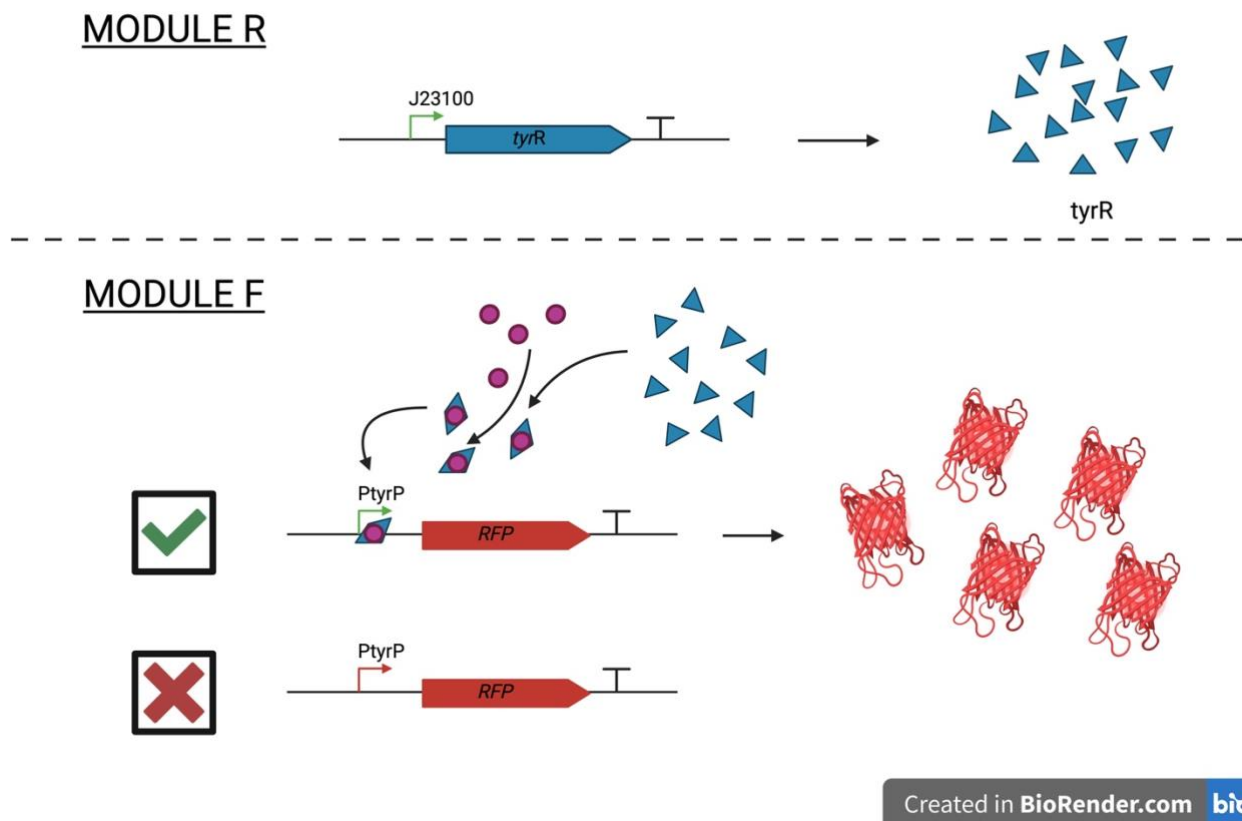


Figure 2. MODULE F + R behavior. **Top.** Module R expresses the *tyrR* protein under the control of a constitutive promoter. **Bottom.** Once the phenylalanine molecules (purple circles) bind to the *tyrR* protein (blue triangles), a dimer is formed, which in turn binds to the *tyrP* promoter activating the transcription of the system. In the absence of phenylalanine, the construct remains inactive, with no detectable signal from the reporter protein.

To obtain incremental signal for Tyr detection, we placed two antisense RNA (asRNA) molecules under the control of the *paroF* promoter. We designed five different asRNAs sequences following previously defined rules and the use of Nupack Software (<https://www.nupack.org>) for calculating the ΔG complex formation (free energy of the mRNA/asRNA complex). This asRNA with different parameters (Table 2) were design in a tailing way covering the UTR (Untranslated region) 5' of the mRNA containing the STAR-*amilGFP* sequence (Hoyne-O'Connor & Moon,

2016b). Two asRNAs were used to bind a) the STAR-regulator RNA, and b) the *amilGFP* RNA. Thus, the transcription of the asRNA will be active in the absence of Tyr and repressed once the TyrR protein binds to Tyr and forms a hexamer, which in turn will bind to the Tyr boxes on the *paroF* promoter, inhibiting the transcription of any gene under its control, in this case, the asRNAs described earlier. In this way, the detection of tyrosine will be converted into an incremental, measurable signal, generated by the reporter that is under the regulation of the STAR sequence and the asRNAs under the *paroF* promoter (Figure 3). For proper development and handling of the system, we split the whole biosensor in different modules, having the module R (Regulatory), F (Phenylalanine) and T (Tyrosine). *Module R* is composed of the transcriptional units of the STAR-regulator and the TyrR protein, both controlled by the *J23100* constitutive promoter. *Module F* was made mainly by the transcriptional unit of the *tyrP-EfordRed* biosensor, and *Module T* was formed for the *paroF-STAR-amilGFP* (Figure 1).

TABLE 2. RESULTS OF ASRNA DESIGNED AGAINST AMILGFP CASSETTE

Name	DNA sequence	RNA sequence	Length	Localization	ΔG free energy kcal/mol	Mismatch %
<i>as1. amilGFP</i>	GAATTCATGT TTACCTCCTA AGGTCTCTAG TA	GAAUUCAUGU UUACCUCCUA AGGUCUCUAG UA	32	USD + SD	-51.93	0
<i>as2. amilGFP</i>	TAAGACATGA ATTCATGTTT ACCTCCTAAG GTCTCTAG	UAAGACAUGA AUUCAUGUUU ACCUCCUAAG GUCUCUAG	38	USD + SD + AUG	-61.49	0
<i>as3. amilGFP</i>	TTTGCTATAA GACATGAATT CATGTTTACC TCCTAAGG	UUUGCUAUAA GACAUGAAUU CAUGUUUACC UCCUAAGG	38	SD + AUG	-59.41	0
<i>as4. amilGFP</i>	AATGCCGTGT TTGCTATAAG ACATGAATTC ATGTTTAC	AAUGCCGUGU UUGCUAUAAAG ACAUGAAUUC AUGUUUAC	38	AUG + C2-8	-61.49	0
<i>as5. amilGFP</i>	TCATTTCTCTG TACAATGCCG TGTTTGCTAT AAGACATG	UCAUUUCCUG UACAAUGCCG UGUUUGCUAU AAGACAUG	38	AUG + C2-8	-62.54	0

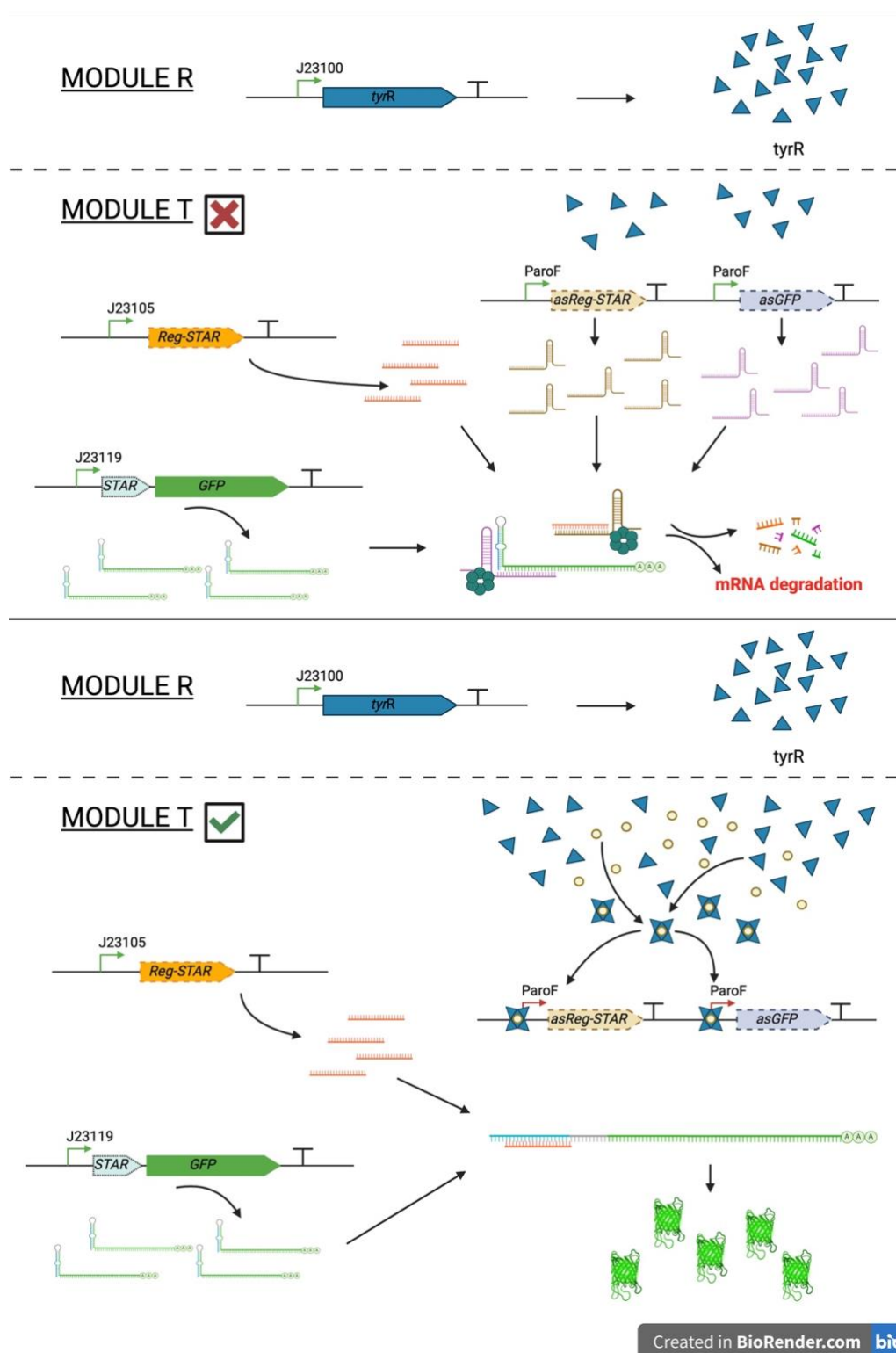


Figure 3. MODULE T + R behavior. **Top:** In the OFF state, the *tyrR* protein stays as a monomer in the absence of tyrosine. The *asRNA* molecules in brown and purple, bind to the *STAR* regulator RNA in orange and the *STAR-GFP* transcript in green respectively, causing the degradation of these complexes by Hfq/RNase activation. **Bottom:** once tyrosine in yellow is present, the *tyrR* proteins acquire a hexamer conformation and block the *paroF* promoters stopping the transcription

of the asRNA molecules, thus releasing the function of the STAR regulator and consequently activating transcription of the STAR-GFP cassette.

***In-vitro*: Molecular Assembly.**

To generate the constructs designed for this biosensor, we followed the steps described on Figure 4-6, using the sequences from Table 1&2, and primer sequences from Table 3 to amplify genomic sequences from *Escherichia coli* K-12 and reporters from Stanford Free Genes (<https://stanford.freegenes.org>). All PCR amplifications were carried out using Hi-Fi Phusion polymerase (Thermo Fisher Scientific). For the different cloning steps, we used Fast Digest restriction enzymes (Thermo Fisher Scientific), or Gibson Assembly (New England Biolabs) as specified on the maps shown in Figure 4-6. For transformations we used *Escherichia coli* DH5α with the classic CaCl₂ chemical transformation protocol (Hannan protocol).

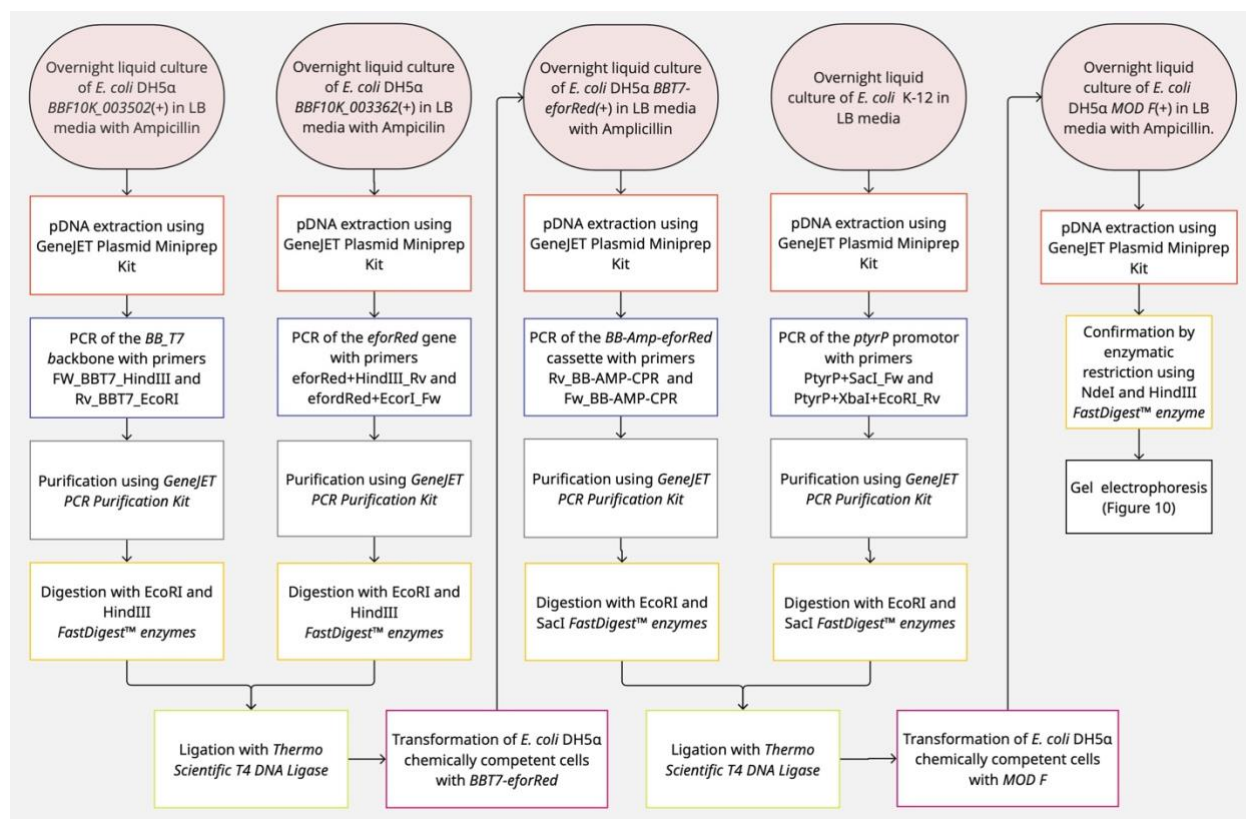
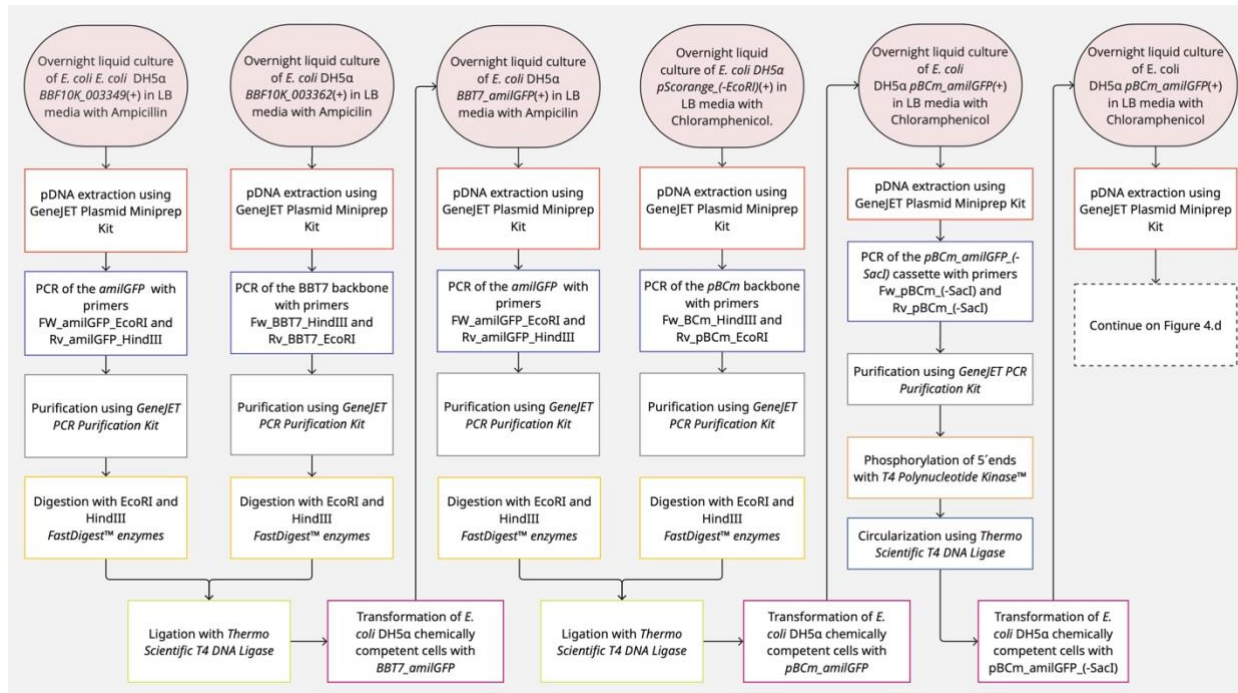
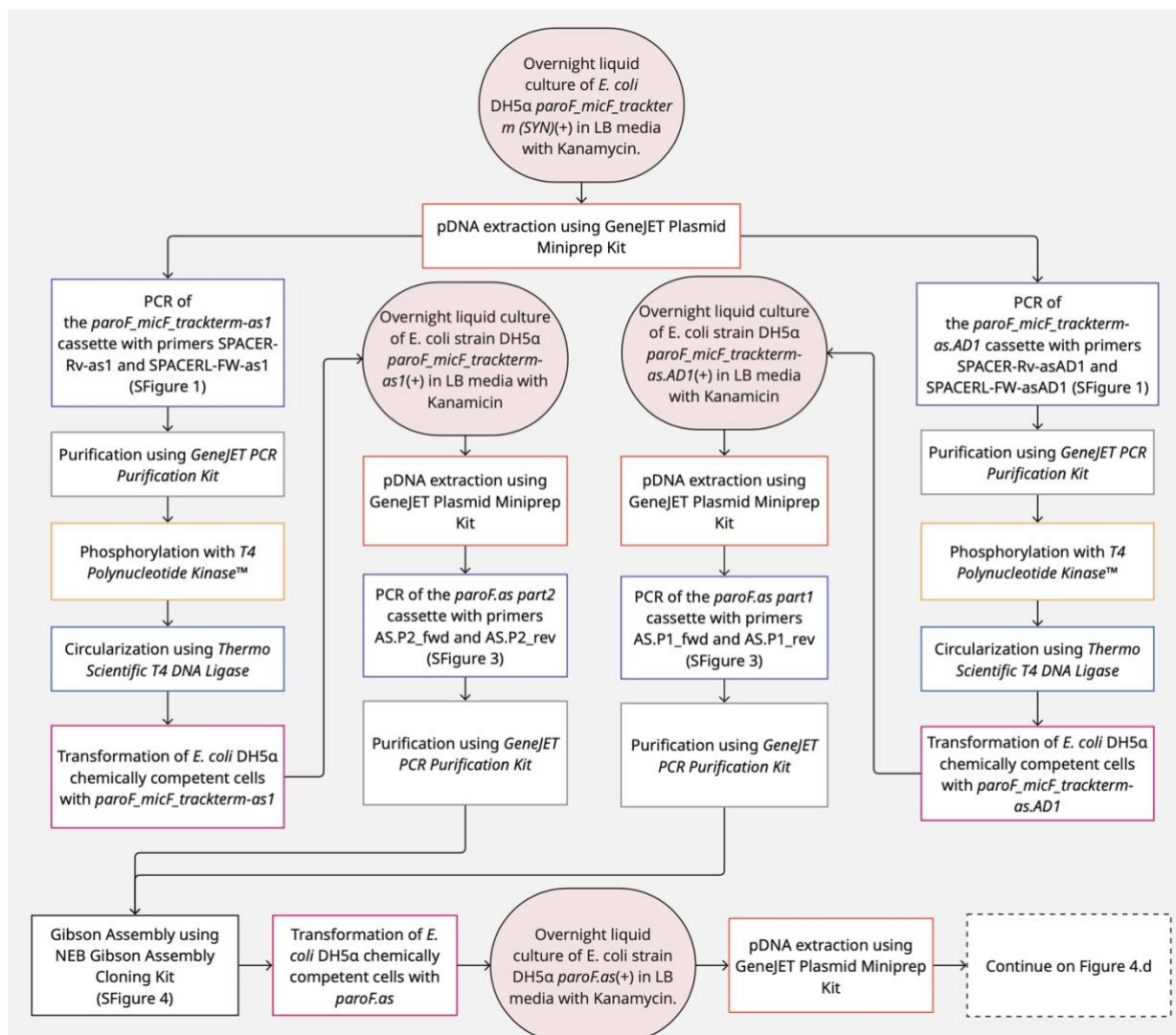


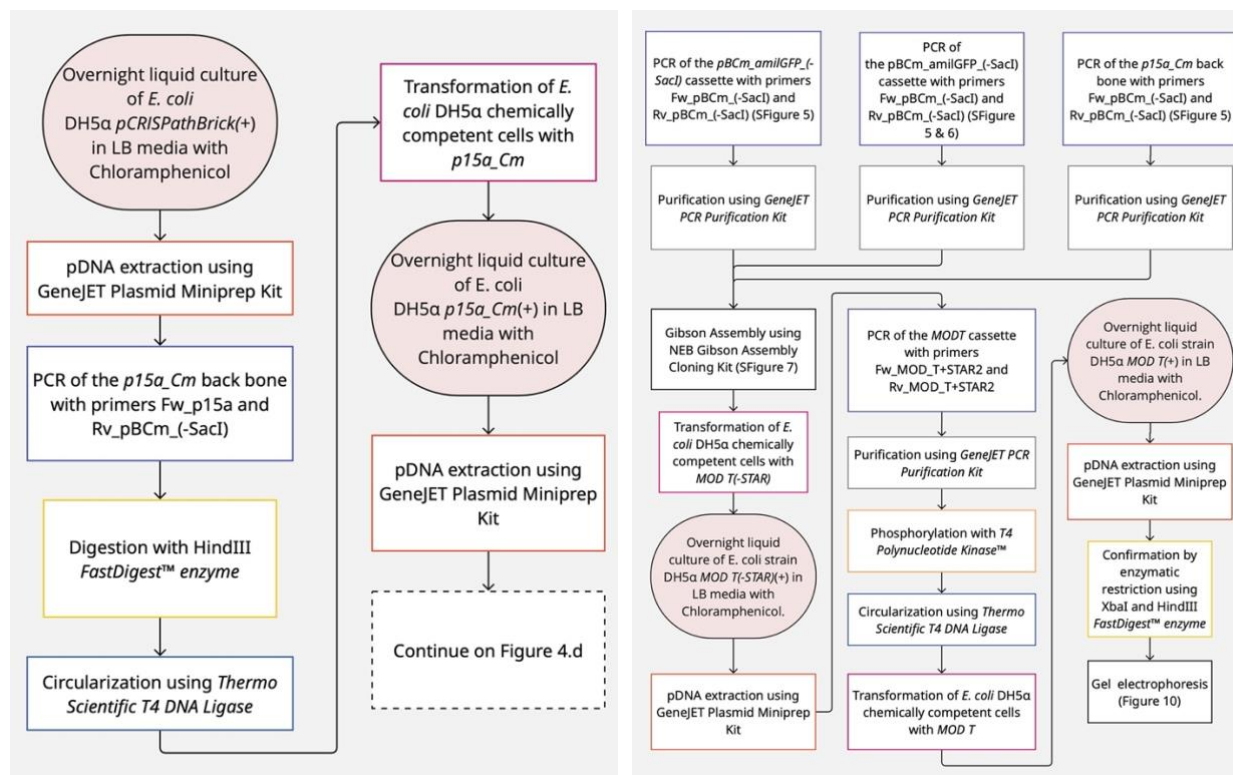
Figure 4. Scheme of *in-vitro* construction of Module F. *In-vitro* steps performed in lab to obtain the *MOD F* plasmid DNA.



a)



b)



c)

d)

Figure 5. Scheme of *in-vitro* construction of Module T. *In-vitro* steps performed in lab to obtain intermedium plasmids a) *pBCm_amilGFP*, b) *paroF.as*, c) *p15a_Cm* and d) final plasmid of *MOD T*

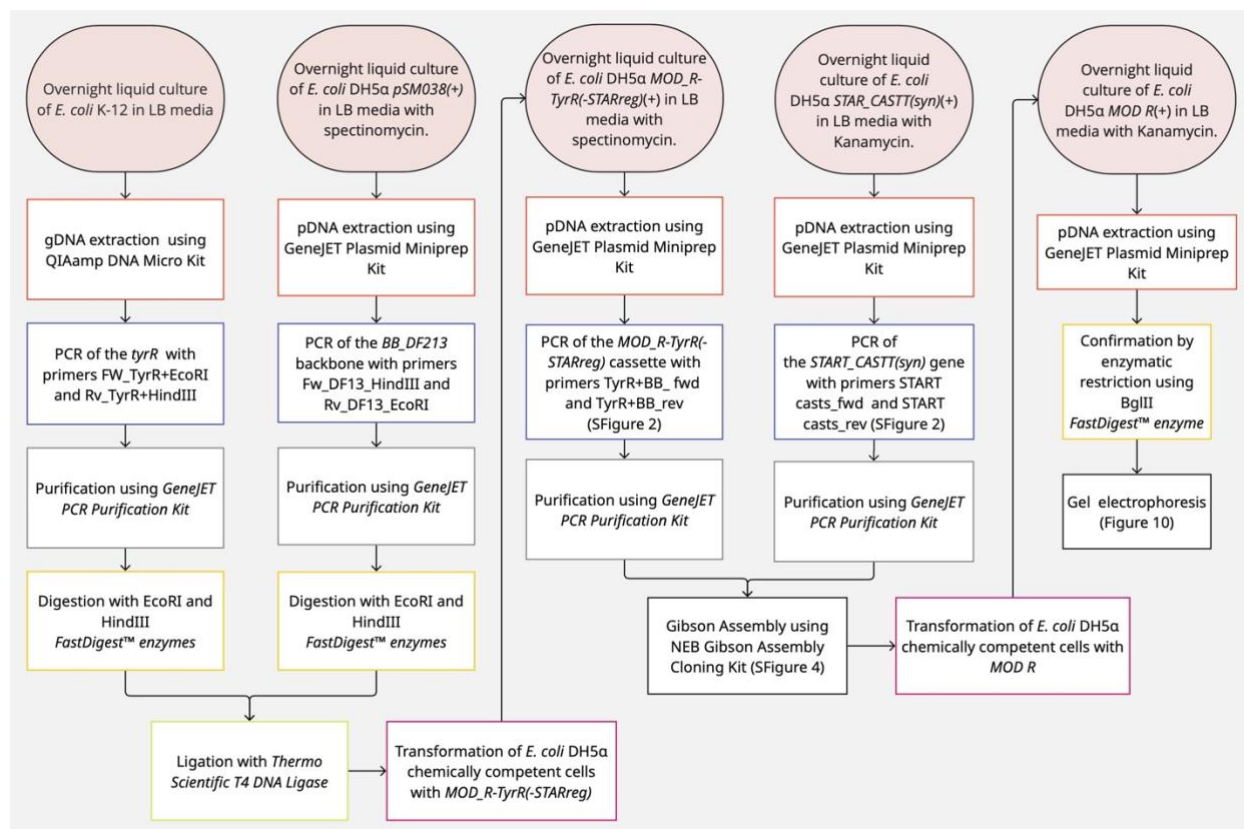


Figure 6. History of *in-vitro* construction of Module R. *In-vitro* steps performed in lab to obtain the *MOD R* plasmid DNA.

TABLE 3. PRIMER SEQUENCES USED IN THIS STUDY

Name	Sequence
Fw_DF13_HindIII	CCAGAAAGCTTCCTAGAGCTAGAGTGCG
Rv_DF13_EcoRI	CGCATGAATTCTATCTACGACCTCCGAC
Fw_TyrR+EcoRI	AGATAGAATTCATGCGTCTGGAAGTCTTTTGT
Rv_TyrR+HindIII	CTAGGAAGCTTAGCTCTGGCTGTACTGAAAGC
TyrR+BB_fwd	TTTTTATTGATAACAAAAACCCCATACGATATAAGTTGTA ATTCTC
TyrR+BB_rev	GACTGAGCTAGCCGTAAATCGAAAAGATCAAAGGATCTT CTTG
START casts_fwd	GAAGATCCTTTGATCTTTTCGATTTACGGCTAGCTCAGTC
START casts_rev	TACAACTTATATCGTATGGGGTTTTTGTATCAATAAAAA AGGCC
Fw_BBT7_HindIII	TTTGAGAAGCTTGATACATAGATTACCACAACCTCC
Rv_BBT7_EcoRI	TGCCATGAATTCTCTCCTTCTTAAAGTTAAACAAAATTAT TTC
eforRed+HindIII_Rv	TGTATCAAGCTTAAAGCTCTTCATGGCAGTGCTTTTCG
eforRed+EcoRI_Fw	AGGAGAGAATTCATGTCCGTGATTAAACAGG
Rv_BB-AMP-CPR	TAGGCTGAGCTCCTTCCGGTGG
Fw_BB-AMP-CPR	ATGCGTCCGGCGTAGAGGATCG
PtyrP+SacI_Fw	TTTTTGAGCTCAGCCTAGCGTAGCGATTGC

PtyrP+XbaI+EcoRI_Rv	TTTTTGAATTCTCTAGAGCTTTCTTCTGTCCTGACGATCTT TATGAG
Fw p15A Cm HindIII	ATCCGAAGCTTGGCTGACTTCAGGTGC
Rv p15A Cm HindIII	CAGCCAAGCTTCGGATCTGCATCGCAG
p15a_fwd	CTTCGCGTTATGCAGGCTTCAATATTTTATCTGATTAATA AGATGATCTTCTTG
p15a_rev	TCACTAAGTGAGGAAACCGCTTCCGGTAGTCAATAAACC G
SPACER-RV-as1	AGGAGGTAAACATGAATTCGCGATAGTTGATCCTCAGCG AGGATG
SPACERL-FW-as1	AAGGTCTCTAGTAGAGCTCTCATTTCTGAATGTCTGTTTA CCCCTATTTCAACCGG
SPACER-RV-asAD1	CTGCTCCAACATTTATACAACGCGATAGTTGATCCTCAGC GAGGATG
SPACERL-FW-asAD1	CGGGGAATGTATACAGTTCATCATTTCTGAATGTCTGTTT ACCCCTATTTCAACCGG
AS.P1_fwd	TATCTGTTCTGCTTCCTCGGCGGTTTCCTCACTTAGTGAT G
AS.P1_rev	TTTACACTCCCTTTGCAAAATACGCAAAAAAAGCACCGA C
AS.P2_fwd	GTCGGTGCTTTTTTTTGCGTATTTTGCAAAGGGAGTGTA TTATC
AS.P2_rev	TCACTAAGTGAGGAAACCGCCGAGGAAGCACGAACAGA TAG
paroF.as_fwd	CGGTTTATTGACTACCGGAAGCGGTTTCCTCACTTAGTGA TG
paroF.as_rev	TAACTGCCGTACTATACGCAAAAAAAGCACCGACTCGGT G
Fw_amilGFP EcoRI	AGGAGAGAATTCATGTCTTATAGCAAACACGGC
Rv_amilGFP HindIII	TGTATCAAGCTTCTCTTCACTTCACTTTCAGCG
Fw_pBCm HindIII	AAGAGAAGCTTATTTGCAGTCCGGCAAAAAAG
Rv_pBCm EcoRI	GACATGAATTCATGTTTACCTCCTAAGGTCTC
Fw_pBCm (-SacI)	GATATCAAATTACGCCCCGCCC
Rv_pBCm (-SacI)	CGCTTGGAATCCTGTTGATAGATCC
amil+STAR_fwd	CATAGTAATGTCTATGGCTTTTCTAGAGTTTACGGCTAGC TC
amil+STAR_rev	TATTAATCAGATAAAATATTGAAGCCTGCATAACGCGAA G
Rv_MOD_T+STAR 2	AACTGTATACATTCCCCGCTGCTCCAACATTTATACA AATTAAACAATTCAGTGTAAAACTGCTAGCATTGTAC CTAGGACTGAGC
Fw_MOD_T+STAR 2	CATGTATATATTCCCCGCTTTTTTTTTTACTAGAGACCTTA GGAGGTAAACATGAATTC
M13F	GTAAAACGACGGCCAGT
M13R-pUC(-40)	CAGGAAACAGCTATGAC

Plasmid Confirmation

For the confirmation of the assembly, we used, functional expression assay, restriction enzyme digestion and sanger sequencing.

Once the PJ23110_STAR_AMILGFP were obtained the strain with this cassette and the previous version PJ23110_AMILGFP CASSETTE that lacks the STAR sequence were streaked on a LB agar plate with (0.05 mg/ml chloramphenicol) and culture for 24 hours. Then fluorescence was assessed by observation of the plates under a blue light transilluminator. For confirmation of the asRNA cassettes by Sanger sequencing we amplify by PCR the cassettes with asRNA with the use of M13 commercial sequencing primers. Then the purified amplicons were delivered to Macrogen in Korea. Finally, for confirmation of the final module's restriction enzyme pattern confirmation were performed over 1 hour at 37°C using *NdeI* and *Hind III* for *MOD F*, *XbaI* and *Hind III* for *MOD T* digested with and *BglII* for *MOD T*. Then samples were loaded on a 1% agarose gel and run at 90mV for 1 hour.

System induction.

Amino Acid Induction Quantification.

For amino acid quantification we prepared DM medium (0.24 mg/mL MgSO₄, 0.3 mM thiamine hydrochloride and 0.4% glucose). Antibiotics were added depending on the strain tested and the different plasmids combinations: *Module T* (0.05 mg/ml chloramphenicol), *Module F* (0.1mg/ml Ampicillin) and *Module R* (Spectinomycin 0.1 mg/ml). *E. coli* cells were grown overnight at 37 °C until saturation. Then, cells were diluted in a 1:50 proportion with fresh DM medium. Amino acid stocks were prepared at 100X concentration. Phenylalanine was prepared with type I water and stored at 100mM, 50mM, 10mM, 5mM, 2.5mM, 1mM, 0.5mM and 0.1mM. Tyrosine was dissolved twice in NaOH and stored at 10mM, 5mM, 2.5mM, 1mM, 0.5mM and 0.1mM. For the experiments, 2µl of the amino acid stocks at different concentrations were added to complete a working volume of 200ul in triplicate. After 24-hour incubation, fluorescence was read using a Qubit4 fluorometer using the blue channel (470nm). Values were normalized using OD₆₀₀ which

was read using a plate reader Epoch I. OD₆₀₀ measurements were used to correct fluorescence values by dividing the blanked absorbance by the blanked fluorescence values. Then, for correcting the background fluorescence, *E. coli* DH5 α cell were grown in same conditions as 0 mM of the amino acids, and measurements were used for correction. Finally, for data visualization, bar charts were plotted, and error bars were calculated. The linear correlation R^2 was also calculated for each treatment.

RESULTS AND DISCUSSION

In-silico and in-vitro validation

We have successfully achieved an *in-silico* design and proposed multiple construction steps that are summarized in Figures 4 to 6. In total, we performed twenty PCRs reactions, four 5' phosphorylations, nine enzyme restriction digestions, nine ligations and three Gibson assembly reactions that were performed according to manufactures instructions. This allowed us to construct the three different modules with a total of 2994bp for *MOD F*, 3562bp for *MOD T* and 3873bp for *MOD R*. From the antisense RNA molecules designed, we selected the as.amilGFP1 sequence based on the parameters obtained, since this structure had a good free energy and a great localization (Table 2 y Figure 7). This molecule contains a sequence complementary to the ribosome binding site (Shine-Dalgarno sequence) present in the target transcript, thus inducing an allosteric block of translation, impeding ribosome binding to the STAR-amilGFP mRNA. In contrast, the asRNA as.amilGFP2 that had a binding affinity greater than the as.amilGFP1, spans all over the USD (Upstream Shine-Dalgarno), SD and AUG parts. However, we followed the same recommendations of Meyer et al. (2015) and included in the design the as.amilGFP1 that spans in the SD directly inside the mRNA molecule and perform this allosteric blockade more efficiently than the as.amilGFP2 which is not located at the center of the SD and leave some free nucleotides in the 5' extreme of the RBS in the transcript. If any of the asRNA molecules from 2 to 5 where

chosen, this could represent a displacement of the blockage and thus not silencing the expression of the transcript. The asRNA as.AD1 where taken from previous work of Lee and collaborators (2018) where they have already validated the functionality of this sequence in similar conditions and usage as ours. For incorporation of the asRNA sequence in site of the *MOD T* plasmids sequences were split in two parts and located as tails in the recombinant primers designed and used for this cloning. Once cassettes *paroF_micF_trackterm-as1* and *paroF_micF_trackterm-as1and as.AD1* were obtained this cassette were sequenced. A 100% identity with the in-silico sequences were obtained (Figure 8 & 9), indicating us that this cloning process was effective and no mutations or scars where introduced.

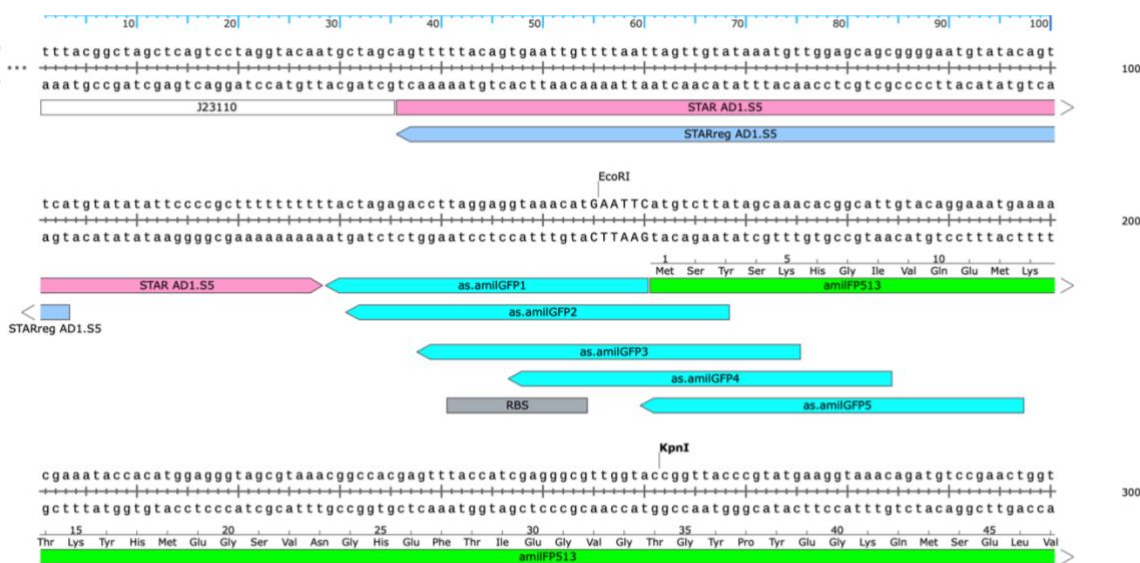
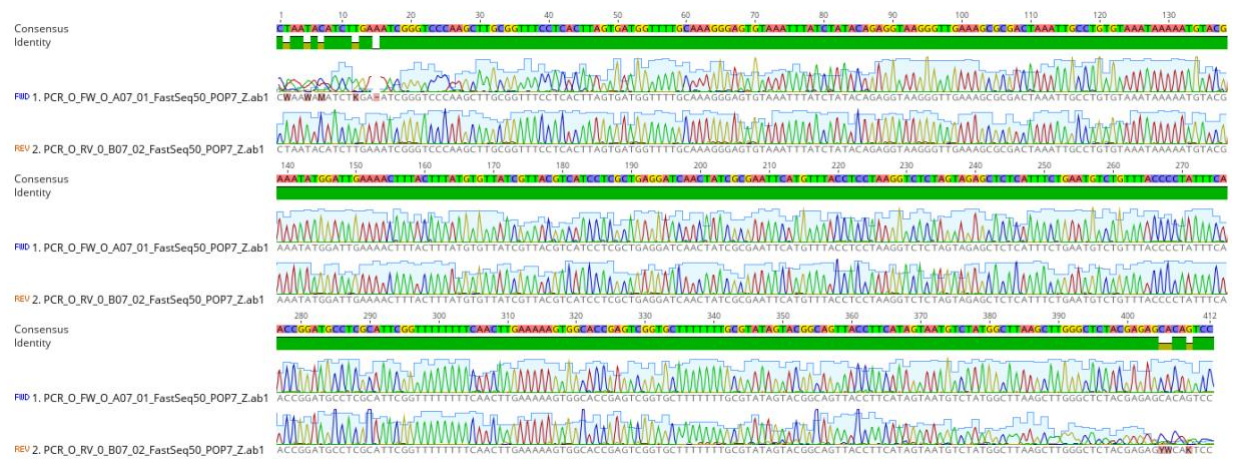
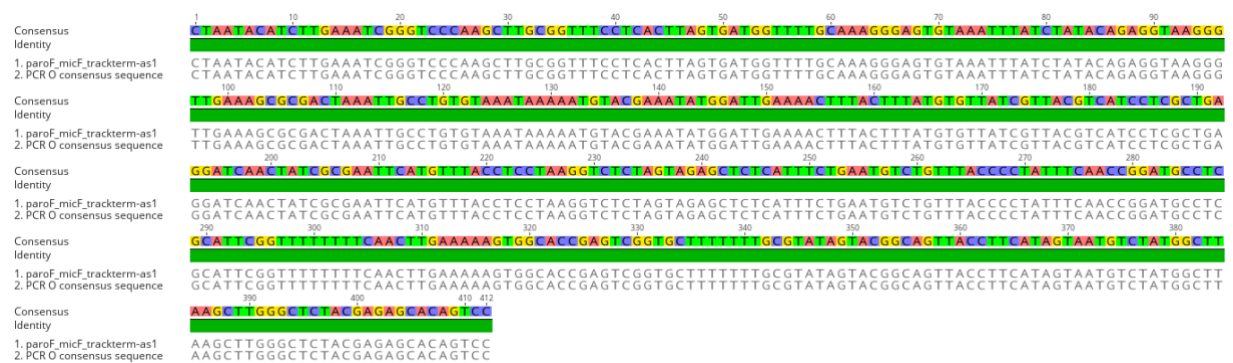


Figure 7. asRNA binding sites for regulation of *STAR-amiGFP* expression cassette. A tiling design of multiple asRNA was generated to achieve tight gene expression control.

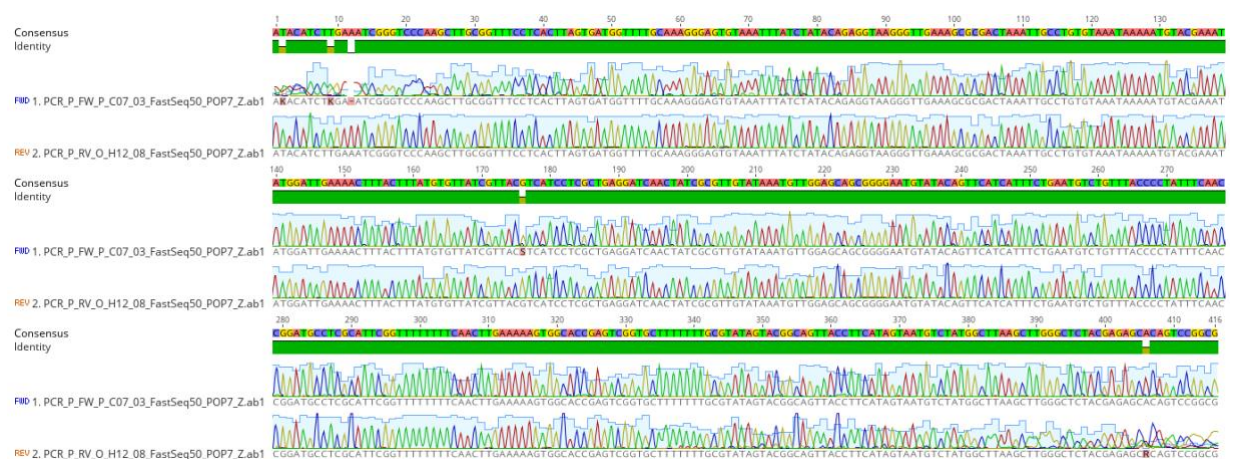


a)

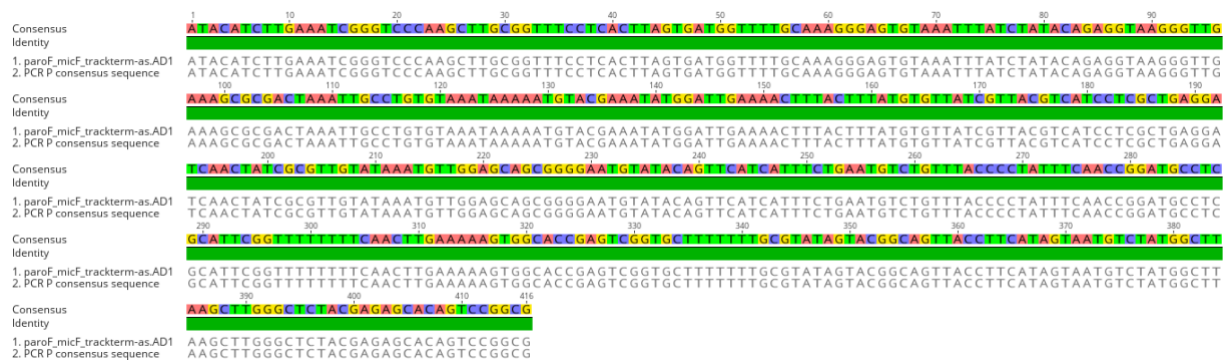


b)

Figure 8. Sanger sequencing confirmation of as1.amilGFP cloning. a) electropherograms of the *paroF_as1.amilGFP_micF_trackterm* cassette. b) confirmation of conservation between *paroF as1.amilGFP micF trackterm* cassette sequenced product and designed sequence.



a)



b)

Figure 9. Sanger sequencing confirmation of as.STAR regulator cloning. a) electropherograms of the *paroF_as.STAR regulator_micF_trackterm* cassette. b) confirmation of conservation between *paroF_as.STAR regulator_micF_trackterm* cassette sequenced product and designed sequence alignment.

To assess the functionality of the *STAR sequence* on the system, we evaluated the repression of this sequence when placed in the *amilGFP* expression cassette in between of the *J23110* promoter and the SD next to the *amilGFP CDS* (Figure 10). Before this addition we had a GFP expressing strain as seen in Figure 10, once this sequence was added fluorescence were repressed. This is due to the activity of this premature terminator formed by the *STAR sequence* that blocks the transcription of this the *amilGFP cassette* (Lee et al., n.d.; Meyer et al., 2015). This bio part known as *AD1.S5* is naturally find in the *pDAI* plasmid of the *Enterococcus faecalis* and its use as a copy number control system (Meyer et al., 2015; Weaver et al., 2004). The counterpart of this part is the *STAR regulator (AD1.S5)* that is an RNA molecule able to bind the 5'extreme of the *STARsequence* and destabilize the hairpin structure, allowing RNA polymerase to transcribe this sequence. The STAR system had been previously designed and domesticated by Meyer and collaborators (2015).

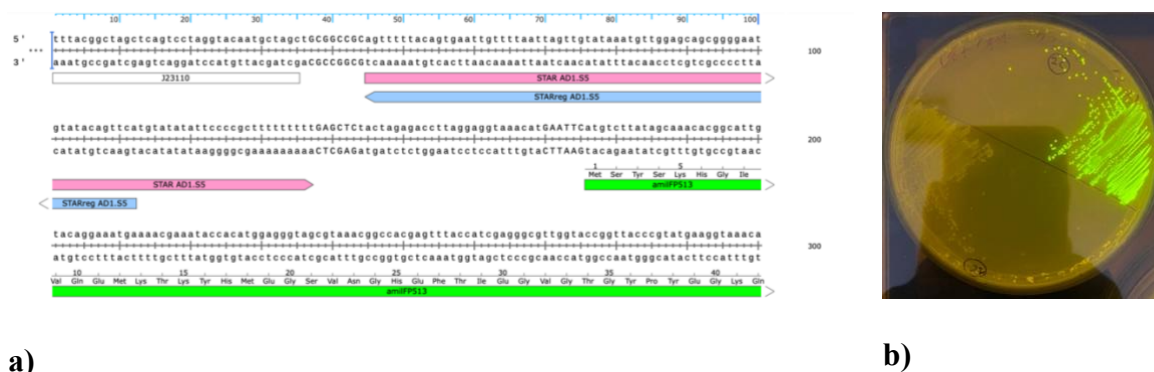


Figure 10. Design and function of *STAR* regulator sequence. a) *In-silico* design of the pJ23110_STAR_amiGFP cassette. b) phenotype of the expression of the pJ23110_STAR_amiGFP cassette (left) and pJ23110_amiGFP cassette (right).

Finally for confirmation of the construction, digestion of the final plasmids were made (Figure 11). *MOD F* were first *in-silico* digested with *NdeI* and *Hind III* what makes two fragments of 2201bp and 793bp, *MOD T* with *XbaI* and *Hind III* making two fragments of 2799bp and 882bp and *MOD T* with *BglIII* making two fragments of 3516bp and 342bp. Once the in-vitro assembled plasmids were digested and runned in an electrophoresis gel, this allows us to see that *MOD F* present two fragments of ≈ 2200 bp and ≈ 800 bp as expected. *MOD R* digestion present two fragments of ≈ 342 bp and ≈ 3516 bp as expected. *MOD T* digested with *XbaI* and *Hind III* present only one fragments between 3000-3200bp, what allows us to think that a deletion was made interfering with *XbaI* or *HindIII* site. When exploring the neighborhood of the restriction sites we can see that there are some possibilities of deletion that could happen in the last assembly steps and still preserve the functionality of the system. One, is the possibility of deletion that could erase the last fragment of the *paroF_micF_trackterm-asI* cassette that has 200bp and presents a repetitive sequence of its bioparts within *paroF_micF_trackterm-as.ADI* cassette, what could represent a problem on primer binding of last PCRs (Figure 12). Further sequencing analysis need

to be performed to elucidate the final structure of sequence and the deletion inside of *MOD T* plasmid and to confirm no other mutations in the rest of plasmids.

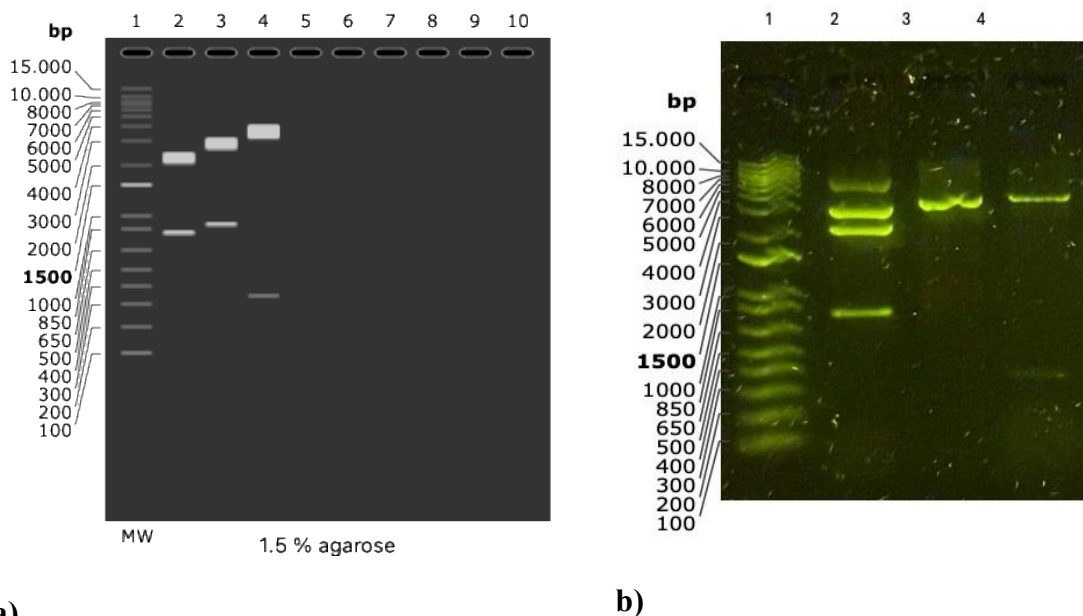


Figure 11. Confirmation of DNA assembly by restriction enzyme digestion. **a)** Expected digestion patter. In lane (1) the S, (2) *MOD F* digested with *NdeI* and *HindIII* making two fragments of 2201bp and 793bp from top to bottom, (3) *MOD T* digested with *XbaI* and *HindIII* making two fragments of 2799bp and 882bp from top to bottom, and (4) *MOD R* digested with *BglII* making 4 fragments of 3516bp and 342bp from top to bottom. **b)** Obtained digestion patter. In lane (1) the Molecular Weight Marker 1Kb Plus from Invitrogen, (2) *MOD F* digested with *NdeI* and *HindIII* making four fragments of ≈ 8000 , ≈ 4000 , ≈ 2201 bp and ≈ 793 bp from top to bottom. First two fragments correspond to a multimer conformation of high copy number plasmid and second to linearized version, (3) *MOD T* digested with *XbaI* and *HindIII* making one fragments of 3000-4000bp, and (4) *MOD R* digested with *BglII* making two fragments of ≈ 3516 bp and ≈ 342 bp from top to bottom.



Figure 12. Neighborhood of selected restriction sites in *MOD T* plasmid. Plasmid map of the MOD T. Different features and architecture of the plasmid are displayed. Note the *HindIII* and *XbaI* sites are displayed in map.

System induction

Once the final plasmids were achieved, two strains were obtained by transforming competent *E. coli* DH5 α cells with *MOD R* + *MOD F* (Phe biosensor) or *MOD R* + *MOD T* (Tyr biosensor). To determine the type of response of the two systems in presence of phenylalanine or tyrosine we set an induction experiment. For the Phe biosensor we obtained data from red fluorescence and OD₆₀₀ from the cells growth with different levels of phenylalanine. For all concentrations, different stocks at 100X concentration were used to achieve final concentrations from 5 μ M to 1000 μ M. The 0 μ M concentration was Type I water, the same solvent used for resuspended and diluted the phenylalanine. As shown in Figure 13 the red fluorescence intensity increase following the increase of Phe concentrations. Furthermore, the correlation with the concentration in the

induction folds presents a linear behavior with the concentration of phenylalanine ($R^2= 0.9021$ in a 5mM to 1000uM concentration range).

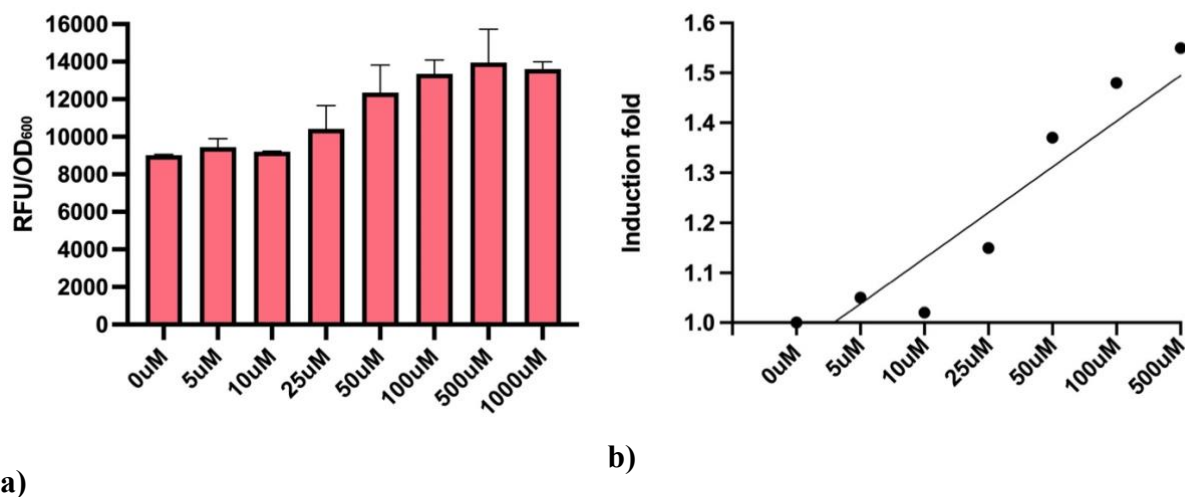


Figure 13. Phenylalanine induction with the Phe-biosensor (*MOD F* + *MOD R*). a) Dose response curves to phenylalanine concentrations and b) linear ranges of Phe-biosensor from 0uM to 500uM.

We also had obtained green fluorescence and OD₆₀₀ measurements from the Tyr biosensor. For this, we use final concentrations from 5uM to 100uM using 100x concentrated stocks. The 0uM concentration was NaOH 0.1M, that is the solvent used for resuspended and diluted tyrosine stocks. As shown in Figure 14 the green fluorescence intensity increases along with the tyrosine concentration tested and as well as in the phenylalanine biosensor the induction fold presents a linear behavior with the concentrations of tyrosine ($R^2= 0.9470$ in a 5nM to 100uM concentration range).

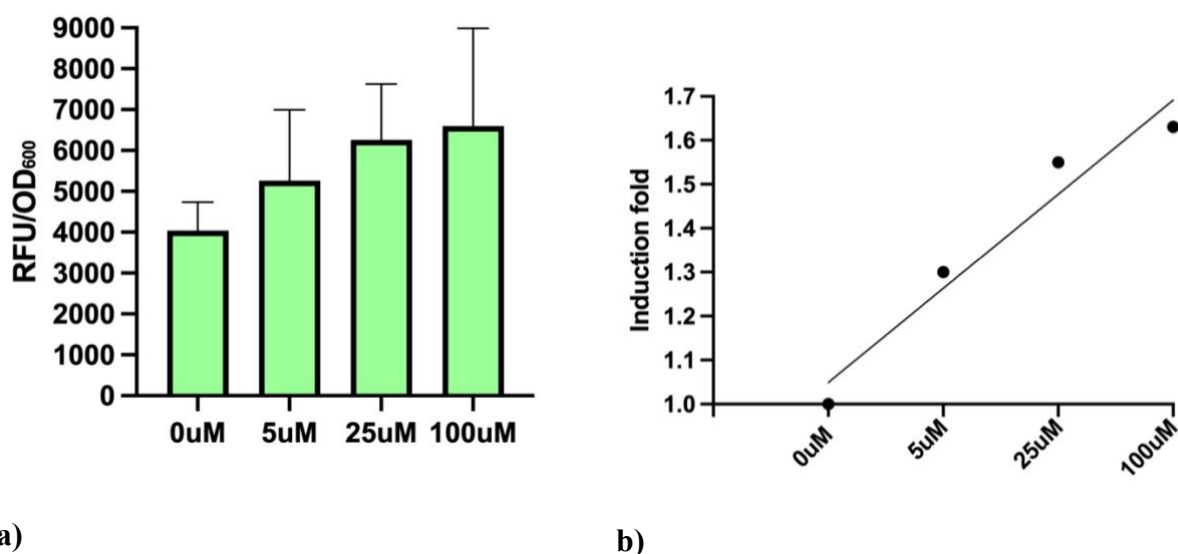


Figure 14. Tyrosine induction with the Tyr-biosensor (*MOD T* + *MOD R*). a) Dose response curves to tyrosine concentrations and b) linear ranges of Tyr-biosensor form 0uM to 100uM.

Both biosensors expose quantifiable and differential levels of fluorescence between the samples. Moreover, the intensity of the system was not enough to be detected with the naked eye. This could be due to low levels from the tyrR protein caused by the use of a *lacIq* strong promoter to express this protein. This represents an expression problem, since high yields of big proteins tend to form inclusion bodies and activate cellular stress responses such as the heat shock response (HSR) and the unfolded protein response (UPR). The accumulation of misfolded TyrR could have led to the activation of proteolytic degradation pathways via Lon and ClpP proteases, reducing the functional protein levels available for transcriptional regulation (Baneyx & Mujacic, 2004).

Furthermore, the formation of inclusion bodies could have lowered the bioavailability of the protein, leading to suboptimal activation of the biosensor system. This phenomenon has been observed in recombinant protein production, where overexpression often results in aggregation and poor solubility, ultimately decreasing the effective concentration of the target protein (Sørensen & Mortensen, 2005). The misfolding and aggregation could have also induced oxidative stress, activating detoxification mechanisms such as superoxide dismutase (SodA) and

catalase (KatG), which are commonly upregulated under protein overexpression stress (Imlay, 2013). To overcome these challenges, future optimizations could include using inducible promoter (T7) weaker promoters or adjusting induction conditions to promote proper folding and solubility of the TyrR protein, improving biosensor performance (Bai et al., 2019a; Lin et al., 2018a; Liu et al., 2017; Mahr et al., 2016; Summers, 1991). The sensibility of the Tyr biosensor could be also enhanced by using strong promoters on the *STAR-amilGFP* and the *STAR regulator* expression cassettes. These two cassettes are controlled under the *J23110* and *J23105* promoters respectively, and inside of the J family members of synthetic promoters, these two exhibit a comparable medium strength if compared with the other members of the Anderson Library (<https://parts.igem.org/Promoters/Catalog/Anderson>). The selection of this promoters, was addressed in this way to ensure molar ratios of these two RNAs populations since these two interact between each other, being the RNA of STAR regulator the one that exhibits its binding activity over the STARsequence (premature terminator) in the *STAR-amilGFP* cassette (Lee et al., n.d.; Meyer et al., 2015). Despite low levels of fluorescence were detected in these preliminary experiments, this can be enhanced by the changes proposed on the promoter sequences. Also, sequencing of all system should be addressed in the next steps to confirm the sequence and structure integrity. Finally, these data show that both biosensors work between the range of relevant physiological levels (Table 4) what makes this circuit a promising technology in a future use as a biosensor for point of care applications and clinic diagnostics.

TABLE 4. PHENYLALANINE AND TYROSINE LEVELS IN NORMAL AND PKU PATIENTS

Fluid	AA	Normal	Moderated PKU	Severe PKU
Sangre	Phenylalanine	40 - 120	600 - 1000	> 1200
	Tyrosine	50 - 100	10 - 30	5 - 10
Orina	Phenylalanine	< 10	~ 500	~ 1000
	Tyrosine	< 10	10 - 20	10 - 20

Reference: Rifai, N., Horvath, A. R., & Wittwer, C. T. (2014). Clinical Chemistry and Molecular Diagnostics. In *Elsevier*.

CONCLUSIONS

In summary, after an intricate design and construction process, a first version of the three-module biosensor for detection of phenylalanine and tyrosine have been developed using transcriptional factors mechanism like the one found in the TyrR protein and the use of antisense ARN technologies. This asRNA were successfully design to redirect the repressive nature of the promoter *paroF* signal that exhibits an inversely proportional signal and tuning it in a directly proportional measurable manner. This promising technology could significantly improve the health of phenylketonuria patients by providing them with a potential tool for a constant monitoring and real time interventions. In this way, our technology could also be applied in the future as a cell free reaction and being put inside of a common rutinary medical device like a urine sample container, as a test strips and even inside of a diaper making a perfect wearable device for pediatric usage

REFERENCES

- Aguirre, A. S., Haro, E., Campodónico, A., Arias-Almeida, B., Mendoza, A., Pozo-Palacios, J., & Aguilar, V. I. R. (2024). Expanding diversity within phenylketonuria in ecuadorian patients: genetic analysis and literature review of newborn screenings. *BMC Pediatrics*, 24(1). <https://doi.org/10.1186/s12887-024-05140-z>
- American College of Medical Genetics. (2009). *Phenylalanine Elevated* (Vol. 2009).
- Bai, D., Ding, D., Li, J., Cong, L., & Zhang, D. (2019a). Pinpointing the l-phenylalanine binding sites of TyrR using biosensors and computer-aided simulation. *Biotechnology Letters*, 41(3), 401–408. <https://doi.org/10.1007/s10529-019-02645-x>
- Bai, D., Ding, D., Li, J., Cong, L., & Zhang, D. (2019b). Pinpointing the l-phenylalanine binding sites of TyrR using biosensors and computer-aided simulation. *Biotechnology Letters*, 41(3), 401–408. <https://doi.org/10.1007/s10529-019-02645-x>
- Baneyx, F., & Mujacic, M. (2004). Recombinant protein folding and misfolding in *Escherichia coli*. *Nature Biotechnology*, 22(11), 1399–1408. <https://doi.org/10.1038/nbt1029>
- Bao, L., Menon, P. N. K., Liljeruhm, J., & Forster, A. C. (2020). Overcoming chromoprotein limitations by engineering a red fluorescent protein. *Analytical Biochemistry*, 611. <https://doi.org/10.1016/j.ab.2020.113936>
- Brown, M. C. J., & Guest, J. F. (1999). Economic impact of feeding a phenylalanine-restricted diet to adults with previously untreated phenylketonuria. *Journal of Intellectual Disability Research*, 43(1), 30–37. <https://doi.org/10.1046/j.1365-2788.1999.43120176.x>
- Castro, I. P. S., Borges, J. M., Chagas, H. A., Tibúrcio, J., Starling, A. L. P., & De Aguiar, M. J. B. (2012). Relationships between phenylalanine levels, intelligence and socioeconomic status of patients with phenylketonuria. *Jornal de Pediatria*, 88(4), 353–356. <https://doi.org/10.2223/JPED.2175>
- Chappell, J., Takahashi, M. K., & Lucks, J. B. (2015). Creating small transcription activating RNAs. *Nature Chemical Biology*, 11(3), 214–220. <https://doi.org/10.1038/nchembio.1737>

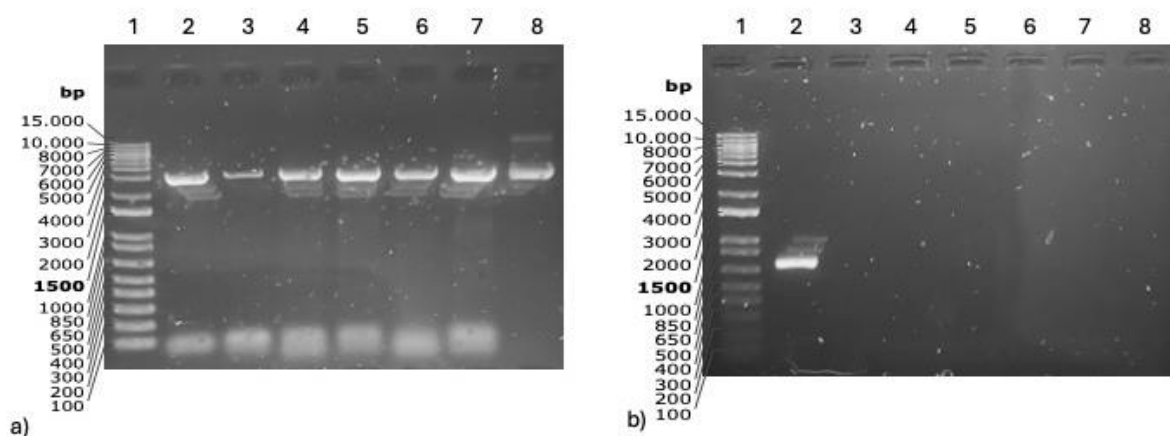
- Chappell, J., Takahashi, M. K., Meyer, S., Loughrey, D., Watters, K. E., & Lucks, J. (2013). The centrality of RNA for engineering gene expression. In *Biotechnology Journal* (Vol. 8, Issue 12, pp. 1379–1395). <https://doi.org/10.1002/biot.201300018>
- Clewell, D. B. (2007). Properties of *Enterococcus faecalis* plasmid pAD1, a member of a widely disseminated family of pheromone-responding, conjugative, virulence elements encoding cytolysin. *Plasmid*, 58(3), 205–227. <https://doi.org/10.1016/j.plasmid.2007.05.001>
- Guo, K. H., Lu, K. H., & Yeh, Y. C. (2018). Cell-Based Biosensor with Dual Signal Outputs for Simultaneous Quantification of Phenylacetic Acid and Phenylethylamine. *ACS Synthetic Biology*, 7(12), 2790–2795. <https://doi.org/10.1021/acssynbio.8b00416>
- Guo, M., Du, R., Xie, Z., He, X., Huang, K., Luo, Y., & Xu, W. (2019a). Using the promoters of MerR family proteins as “rheostats” to engineer whole-cell heavy metal biosensors with adjustable sensitivity. *Journal of Biological Engineering*, 13(1). <https://doi.org/10.1186/s13036-019-0202-3>
- Guo, M., Du, R., Xie, Z., He, X., Huang, K., Luo, Y., & Xu, W. (2019b). Using the promoters of MerR family proteins as “rheostats” to engineer whole-cell heavy metal biosensors with adjustable sensitivity. *Journal of Biological Engineering*, 13(1). <https://doi.org/10.1186/s13036-019-0202-3>
- Haghighi, F., Talebpour, Z., Amini, V., Ahmadzadeh, A., & Farhadpour, M. (2015). A fast high performance liquid chromatographic (HPLC) analysis of amino acid phenylketonuria disorder in dried blood spots and serum samples, employing C18 monolithic silica columns and photo diode array detection. *Analytical Methods*, 7(18), 7560–7567. <https://doi.org/10.1039/c5ay00745c>
- Hoynes-O’Connor, A., & Moon, T. S. (2016a). Development of Design Rules for Reliable Antisense RNA Behavior in *E. coli*. *ACS Synthetic Biology*, 5(12), 1441–1454. <https://doi.org/10.1021/acssynbio.6b00036>

- Hoynes-O'Connor, A., & Moon, T. S. (2016b). Development of Design Rules for Reliable Antisense RNA Behavior in *E. coli*. *ACS Synthetic Biology*, 5(12), 1441–1454. <https://doi.org/10.1021/acssynbio.6b00036>
- Imlay, J. A. (2013). The molecular mechanisms and physiological consequences of oxidative stress: lessons from a model bacterium. *Nature Reviews Microbiology*, 11(7), 443–454. <https://doi.org/10.1038/nrmicro3032>
- Lee, Y. J., Kim, S. J., Amroffell, M. B., & Moon, T. S. (2019). Establishing a Multivariate Model for Predictable Antisense RNA-Mediated Repression. *ACS Synthetic Biology*, 8(1), 45–56. <https://doi.org/10.1021/acssynbio.8b00227>
- Lee, Y. J., Kim, S.-J., & Moon, T. S. (n.d.). *Multilevel regulation of bacterial gene expression with the combined STAR and antisense RNA system*.
- Liljeruhm, J., Funk, S. K., Tietscher, S., Edlund, A. D., Jamal, S., Wistrand-Yuen, P., Dyrhage, K., Gynnå, A., Ivermark, K., Lövgren, J., Törnblom, V., Virtanen, A., Lundin, E. R., Wistrand-Yuen, E., & Forster, A. C. (2018). Engineering a palette of eukaryotic chromoproteins for bacterial synthetic biology. *Journal of Biological Engineering*, 12(1). <https://doi.org/10.1186/s13036-018-0100-0>
- Lin, C., Jair, Y. C., Chou, Y. C., Chen, P. S., & Yeh, Y. C. (2018a). Transcription factor-based biosensor for detection of phenylalanine and tyrosine in urine for diagnosis of phenylketonuria. *Analytica Chimica Acta*, 1041, 108–113. <https://doi.org/10.1016/j.aca.2018.08.053>
- Lin, C., Jair, Y. C., Chou, Y. C., Chen, P. S., & Yeh, Y. C. (2018b). Transcription factor-based biosensor for detection of phenylalanine and tyrosine in urine for diagnosis of phenylketonuria. *Analytica Chimica Acta*, 1041, 108–113. <https://doi.org/10.1016/j.aca.2018.08.053>
- Liu, Y., Zhuang, Y., Ding, D., Xu, Y., Sun, J., & Zhang, D. (2017). Biosensor-Based Evolution and Elucidation of a Biosynthetic Pathway in *Escherichia coli*. *ACS Synthetic Biology*, 6(5), 837–848. <https://doi.org/10.1021/acssynbio.6b00328>

- Mahr, R., von Boeselager, R. F., Wiechert, J., & Frunzke, J. (2016). Screening of an *Escherichia coli* promoter library for a phenylalanine biosensor. *Applied Microbiology and Biotechnology*, 100(15), 6739–6753. <https://doi.org/10.1007/s00253-016-7575-8>
- Matalon, R., & Michals, K. (1991). Phenylketonuria: screening, treatment and maternal PKU. *Clinical Biochemistry*, 24(4), 337–342. [https://doi.org/10.1016/0009-9120\(91\)80008-Q](https://doi.org/10.1016/0009-9120(91)80008-Q)
- MedlinePlus. (2017). *Phenylketonuria*. <https://doi.org/quency>
- Meyer, S. (2015). *Improving fold activation of small transcription activating RNAs (STARs) with rational RNA engineering strategies*. 1–20.
- Meyer, S., Chappell, J., Sankar, S., Chew, R., & Lucks, J. B. (2015). *Improving fold activation of small transcription activating RNAs (STARs) with rational RNA engineering strategies*. <https://doi.org/10.1101/022772>
- Mihali, C. V., Ciolacu, C. F. L., Frențescu, L., Petrescu, C. M., Mândruțiu, I., Bechet, D., Nistor, T., Ardelean, A., & Benga, G. (2018). Determination of plasma phenylalanine concentration by two dimensional thin layer chromatography and high performance liquid chromatography in relation with diagnosis of phenylketonuria. *Studia Universitatis Babes-Bolyai Chemia*, 63(4), 79–94. <https://doi.org/10.24193/subbchem.2018.4.06>
- Navani, N. K., Dhyani, R., Shankar, K., Bhatt, A., Jain, S., & Hussain, A. (2021). Homogentisic acid-based whole-cell biosensor for detection of alkaptonuria disease. *Analytical Chemistry*, 93(10), 4521–4527. <https://doi.org/10.1021/acs.analchem.0c04914>
- Nelwan, M. L. (2020). Phenylketonuria: Genes in phenylketonuria, diagnosis, and treatments. *African Journal of Biological Sciences (South Africa)*, 2(1), 1–8. <https://doi.org/10.33472/AFJBS.2.1.2020.1-8>
- Pittard, J., Camakaris, H., & Yang, J. (2005). The TyrR regulon. In *Molecular Microbiology* (Vol. 55, Issue 1, pp. 16–26). <https://doi.org/10.1111/j.1365-2958.2004.04385.x>
- Rampini, S., Vollmin, J. A., Bosshard, H. R., Muller, M., & Curtius, H. C. (1974). Aromatic acids in urine of healthy infants, persistent hyperphenylalaninemia, and phenylketonuria, before

- and after phenylalanine load. *Pediatric Research*, 8(7), 704–709.
<https://doi.org/10.1203/00006450-197407000-00003>
- Roy, R., Ray, S., Chowdhury, A., & Anand, R. (2021). Tunable Multiplexed Whole-Cell Biosensors as Environmental Diagnostics for ppb-Level Detection of Aromatic Pollutants. *ACS Sensors*, 6(5), 1933–1939. <https://doi.org/10.1021/acssensors.1c00329>
- Sørensen, H. P., & Mortensen, K. K. (2005). Advanced genetic strategies for recombinant protein expression in *Escherichia coli*. *Journal of Biotechnology*, 115(2), 113–128.
<https://doi.org/10.1016/j.jbiotec.2004.08.004>
- Summers, D. (1991). The kinetics of plasmid loss. *Trends in Biotechnology*, 9(1), 273–278.
[https://doi.org/10.1016/0167-7799\(91\)90089-Z](https://doi.org/10.1016/0167-7799(91)90089-Z)
- van Spronsen, F. J., Blau, N., Harding, C., Burlina, A., Longo, N., & Bosch, A. M. (2021). Phenylketonuria. *Nature Reviews Disease Primers*, 7(1), 1–19.
<https://doi.org/10.1038/s41572-021-00267-0>
- Vogel, J., & Luisi, B. F. (2011). Hfq and its constellation of RNA. In *Nature Reviews Microbiology* (Vol. 9, Issue 8, pp. 578–589). <https://doi.org/10.1038/nrmicro2615>
- Watstein, D. M., & Styczynski, M. P. (2018). Development of a Pigment-Based Whole-Cell Zinc Biosensor for Human Serum. *ACS Synthetic Biology*, 7(1), 267–275.
<https://doi.org/10.1021/acssynbio.7b00292>
- Weaver, K. E., Ehli, E. A., Nelson, J. S., & Patel, S. (2004). Antisense RNA Regulation by Stable Complex Formation in the *Enterococcus faecalis* Plasmid *pAD1* par Addiction System. *186*(19), 6400–6408. <https://doi.org/10.1128/JB.186.19.6400>
- Wilson, I. D., Plumb, R., Granger, J., Major, H., Williams, R., & Lenz, E. M. (2005). HPLC-MS-based methods for the study of metabonomics. *Journal of Chromatography B: Analytical Technologies in the Biomedical and Life Sciences*, 817(1), 67–76.
<https://doi.org/10.1016/j.jchromb.2004.07.045>

SUPPLEMENTARY MATERIAL



SFigure 1. PCR of asRNA molecules. **a)** (1) Molecular Weight Marker 1Kb Plus from Invitrogen, (2) *paroF_micF_trackterm_as.ADI*, (3) *paroF_micF_trackterm_as1*, (4) *paroF_micF_trackterm_as2*, (5) *paroF_micF_trackterm_as2*, (6) *paroF_micF_trackterm_as4*, (7) *paroF_micF_trackterm_as5*, (8) DNA template (*paroF_micF_trackterm*(SYN)) **b)** (1) Molecular Weight Marker 1Kb Plus from Invitrogen, (2) positive control *amilGFP*, (3) negative control.

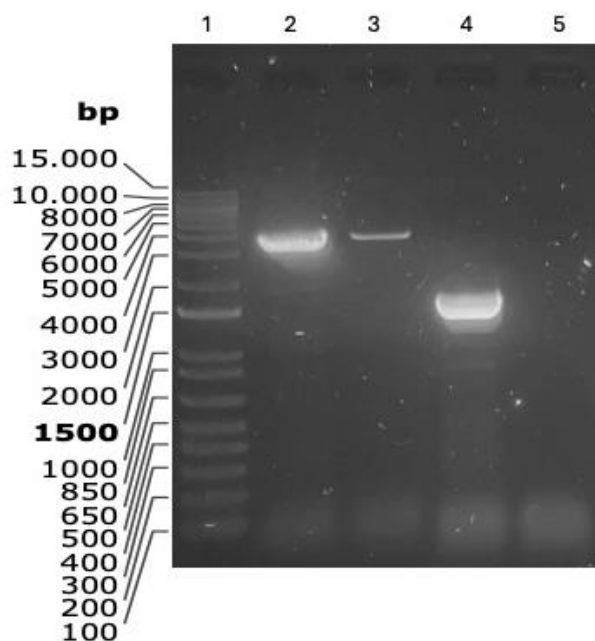


Figure 2. PCR of MOD T parts for Gibson assembly. (1) Molecular Weight Marker 1Kb Plus from Invitrogen, (2) *MOD_R-TyrR(-STARreg)* at 55°C as T_m, (3) *MOD_R-TyrR(-STARreg)* at 68,5°C as T_m, (4) *positive control 16S of E. coli K12*, (5) negative control.

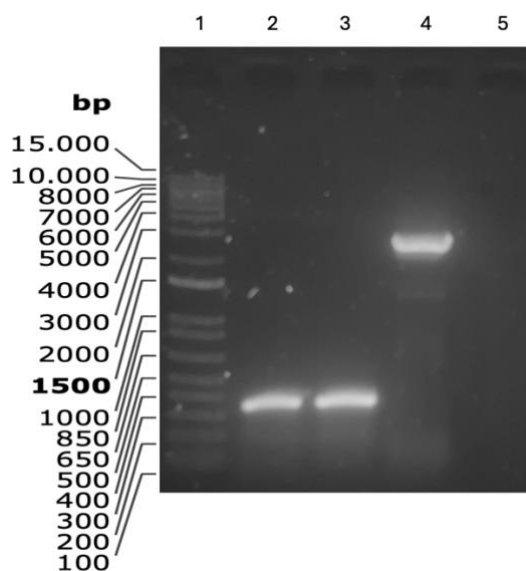


Figure 3. PCR of *paroF.as* parts for Gibson assembly. (1) Molecular Weight Marker 1Kb Plus from Invitrogen, (2) *paroF.as* part 1 at 60°C as T_m, (3) *paroF.as* part 1 at 72°C as T_m, (4) *paroF.as* part 1 at 60°C as T_m, (5) negative control.

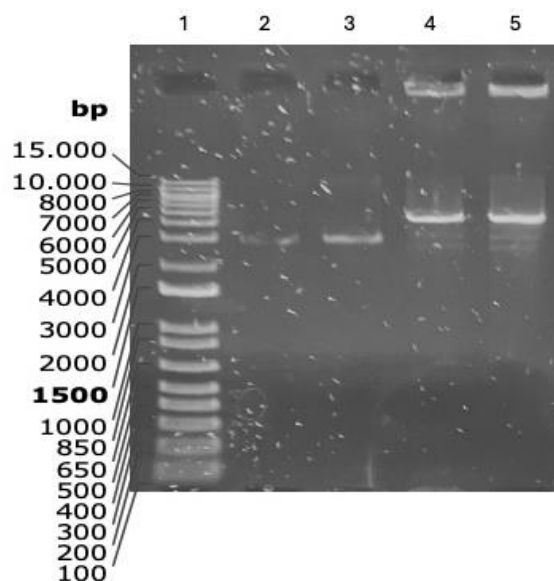


Figure 4. Confirmation of Gibson Assembly by restriction enzyme digestion. (1) Molecular Weight Marker 1Kb Plus from Invitrogen, (2) *EcoRI* linearization of DNA extracted from colony 1 of *paroF.as* transformation, (3) *EcoRI* linearization of DNA extracted from colony 2 of *paroF.as* transformation, (4) DNA extracted from colony 1 of *MOD R* Gibson assembly transformation and linearized with *HindIII*, (5) DNA extracted from colony 2 of *MOD R* Gibson assembly and transformation linearized with *EcoRI*.

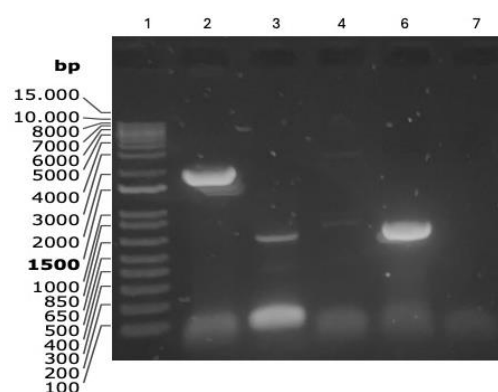


Figure 5. PCR of *MODT(-STAR)* parts for Gibson assembly. (1) Molecular Weight Marker 1Kb Plus from Invitrogen, (2) *p15* backbone, (3) *paroF.as* cassette, (4) *pBCm_amilGFP(-SacI)*, (5) positive control *amilGFP*, (6) negative control.

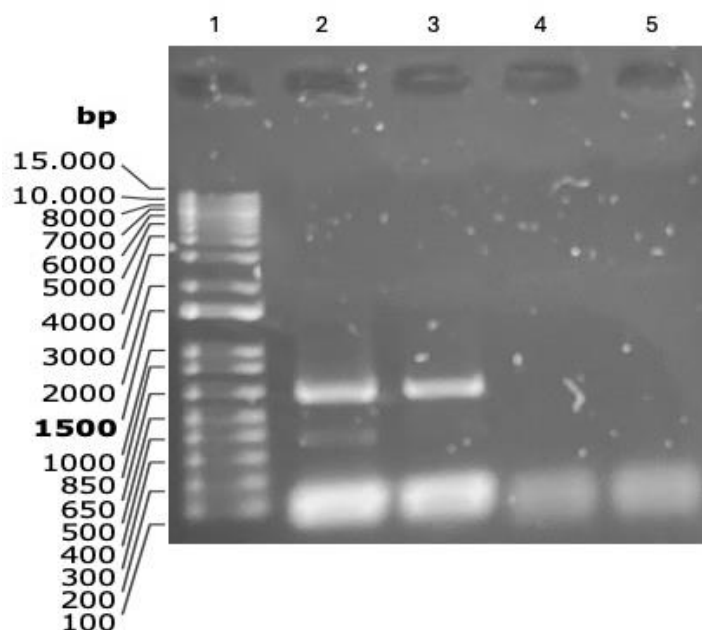


Figure 6. PCR of *MODT(-STAR)* parts for Gibson assembly (2). (1) Molecular Weight Marker 1Kb Plus from Invitrogen, (2) *paroF.as* cassette at 62°C as T_m, (3) *paroF.as* cassette at 72°C as T_m, (4) *pBCm_amilGFP(-SacI)* at 62°C as T_m, (5) *pBCm_amilGFP(-SacI)* at 72°C as T_m.

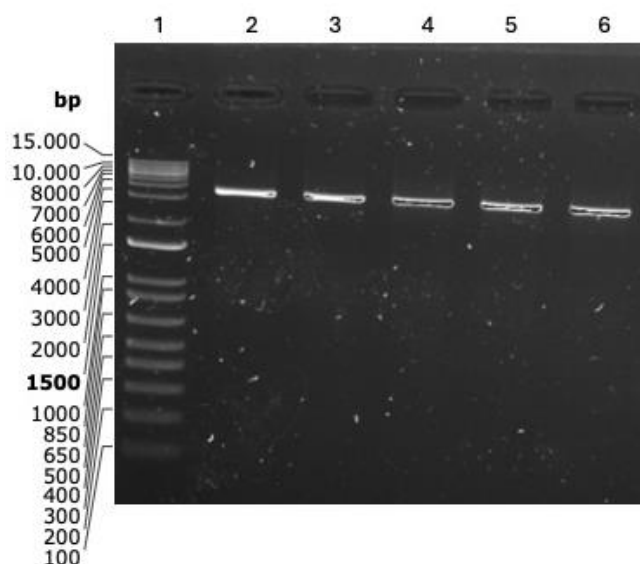


Figure S6. Confirmation of Gibson Assembly by restriction enzyme digestion. (1) Molecular Weight Marker 1Kb Plus from Invitrogen, (2) *HindIII* linearization of DNA extracted from colony 1 of *MODT(-STAR)* transformation, (3) *HindIII* linearization of DNA extracted from colony 2 of *MODT(-STAR)* transformation, (4) *HindIII* linearization of DNA extracted from colony 3 of *MODT(-STAR)* transformation, (5) *HindIII* linearization of DNA extracted from colony 4 of *MODT(-STAR)* transformation.

MODT(-STAR) transformation,(6) *HindIII* linearization of DNA extracted from colony 5 of *MODT(-STAR)* transformation.